

การสังเคราะห์และวิเคราะห์คุณลักษณะของพอลิอิมัลทีไวต์ต่อแสงชนิดเนกาทีฟที่มีความหนาพิเศษ

นางสาวนพมาศ วุฒิกุลประพันธ์

วิทยานิพนธ์นี้เป็นส่วนหนึ่งของการศึกษาตามหลักสูตรปริญญาวิทยาศาสตรมหาบัณฑิต

สาขาวิชาวิศวกรรมเคมี ภาควิชาวิศวกรรมเคมี

คณะวิศวกรรมศาสตร์ จุฬาลงกรณ์มหาวิทยาลัย

ปีการศึกษา 2555

ลิขสิทธิ์ของจุฬาลงกรณ์มหาวิทยาลัย

บทคัดย่อและแฟ้มข้อมูลฉบับเต็มของวิทยานิพนธ์ตั้งแต่ปีการศึกษา 2554 ที่ให้บริการในคลังปัญญาจุฬาฯ (CUIR)

เป็นแฟ้มข้อมูลของนิสิตเจ้าของวิทยานิพนธ์ที่ส่งผ่านทางบัณฑิตวิทยาลัย

The abstract and full text of theses from the academic year 2011 in Chulalongkorn University Intellectual Repository (CUIR)

are the thesis authors' files submitted through the Graduate School.

SYNTHESIS AND CHARACTERIZATION OF ULTRA-THICK NEGATIVE  
PHOTOSENSITIVE POLYIMIDE

Miss Noppamas Wutikunprapan

A Thesis Submitted in Partial Fulfillment of the Requirements  
for the Degree of Master of Engineering Program in Chemical Engineering

Department of Chemical Engineering

Faculty of Engineering

Chulalongkorn University

Academic Year 2012

Copyright of Chulalongkorn University

Thesis Title                   SYNTHESIS AND CHARACTERIZATION OF ULTRA-  
  THICK NEGATIVE PHOTSENSITIVE POLYIMIDE  
By                                 Miss Noppamas Wutikunprapan  
Field of Study                 Chemical Engineering  
Thesis Advisor                Associate Professor M.L. Supakanok Thongyai, Ph.D.

---

Accepted by the Faculty of Engineering, Chulalongkorn University in  
Partial Fulfillment of the Requirements for the Master's Degree

..... Dean of the Faculty of Engineering  
(Associate Professor Boonsom Lerthirunwong, Dr.Eng.)

#### THESIS COMMITTEE

..... Chairman  
(Professor Piyasan Prasertdam, Dr.Eng.)

..... Thesis Advisor  
(Associate Professor M.L. Supakanok Thongyai, Ph.D.)

..... Examiner  
(Assistant Professor Soorathep Kheawhom, Ph.D.)

..... Examiner  
(Assistant Professor Anongnat Somwangthanaroj, Ph.D.)

..... External Examiner  
(Assistant Professor Sirirat Wacharawichanant, D.Eng.)

นพมาศ วุฒิกุลประพันธ์: การสังเคราะห์และวิเคราะห์คุณลักษณะของพอลิอิมิด์ที่ไวต่อแสงชนิดเนกาทีฟที่มีความหนาพิเศษ (SYNTHESIS AND CHARACTERIZATION OF ULTRA-THICK NEGATIVE PHOTSENSITIVE POLYIMIDE) อ.ที่ปรึกษาวิทยานิพนธ์หลัก: รศ. ดร. ม.ล. ศุภกนก ทองใหญ่, 78 หน้า.

พอลิอิมิด์ที่ไวต่อแสงเป็นหนึ่งในโพลิเมอร์ที่น่าสนใจด้านวิศวกรรม โดยเฉพาะอย่างยิ่งสำหรับอุตสาหกรรมไมโครอิเล็กทรอนิกส์ เราศึกษาและสืบหาเงื่อนไขที่เหมาะสมสำหรับการสังเคราะห์พอลิอิมิด์ที่ไวต่อแสงว่าสามารถนำมาใช้เป็นวัสดุที่ขึ้นลายวงจรได้ พอลิอิมิด์ที่ไวต่อแสงชนิดเนกาทีฟสังเคราะห์ได้จากปฏิกิริยาระหว่าง 3,3',4,4'-ไบฟีนิลเตตระคาร์บอกซิลิก ไดแอนไฮดรายด์ กับ เฮกซะเมทิลีนไดเอมีน และ 4,4'-ออกซิไดแอนนิติน โดยใช้อัตราส่วนของไดแอนไฮดรายด์ต่อไดเอมีนเป็น 100:30:70 ในสารละลายนอโมล-เมทิล-2-ไพโรลิดีโนน โดยวิธีพอลิเมอร์ไรเซชันแบบควบแน่นที่อุณหภูมิห้องและอิมิดิเซชันที่ 250 °C ตัวโพลีไดอินนิซิเอเตอร์และโพลีโพรพิลีนไดเอทิลีนที่ใช้เป็น ไอคาเคียว-819 และ 2-ไฮดรอกซีเอทิล เมทาไครเลท ตามลำดับ ในการศึกษาพอลิอิมิด์ที่ไวต่อแสงถูกใช้สำหรับเป็นชั้นฉนวนกันความร้อนที่ควบคุมความหนาของชั้นฟิล์มอยู่ที่ประมาณ 12.5 ไมครอนดังนั้นความหนาของชั้นฟิล์มจึงเรียกว่า “ความหนาพิเศษ” และพื้นที่การเปิดรูของฟิล์มพอลิอิมิด์ที่ไวต่อแสงชนิดเนกาทีฟเป็น 4 ตารางมิลลิเมตร การปรับปรุงพอลิอิมิด์ที่ไวต่อแสงเพื่อลดการหดตัวของฟิล์มหลังจากผ่านกระบวนการอบที่อุณหภูมิสูงทำโดยการสังเคราะห์ฟิล์มพอลิอิมิด์ที่ไวต่อแสงซิลิกาไฮบริด (ออกตะไวเนล พอส) โครงสร้างของพอลิอิมิด์ที่ไวต่อแสงและพอลิอิมิด์ที่ไวต่อแสงซิลิกาไฮบริดนำมาวิเคราะห์โดยใช้ FTIR และ <sup>1</sup>H-NMR ลักษณะทางสัณฐานวิทยาตรวจสอบโดยใช้ Optical และ Confocal Microscope ส่วนความเสถียรทางความร้อนของฟิล์มใช้ TGA และค่าคงที่ไดอิเล็กทริกใช้ LCR meter ในการวิเคราะห์ ซึ่งจากคุณสมบัติเหล่านี้สามารถนำพอลิอิมิด์ที่ไวต่อแสงซิลิกาไฮบริดที่ได้ไปประยุกต์ใช้ในอุตสาหกรรมไมโครอิเล็กทรอนิกส์ได้อย่างมีประสิทธิภาพต่อไป

ภาควิชา.....วิศวกรรมเคมี.....

ลายมือชื่อนิสิต.....

สาขาวิชา.....วิศวกรรมเคมี.....

ลายมือชื่ออ.ที่ปรึกษาวิทยานิพนธ์หลัก.....

ปีการศึกษา.....2555.....

##5470235421: MAJOR CHEMICAL ENGINEERING

KEY WORDS: NEGATIVE PHOTSENSITIVE POLYIMIDE/POLYIMIDE-SILICA  
HYBRID/ULTRA-THICK

NOPPAMAS WUTIKUNPRAPAN: SYNTHESIS AND CHARACTERIZATION  
OF ULTRA-THICK NEGATIVE PHOTSENSITIVE POLYIMIDE. ADVISOR:  
ASSOC.PROF.M.L.SUPAKANOK THONGYAI, Ph.D., 78 pp.

Photosensitive polyimide (PSPI) is one of the great interesting engineering polymers, especially for microelectronic industry. We studies and optimized the synthesis conditions for a PSPI that can be used as lithography material. Negative photosensitive polyimide (NPSPI) have been synthesized by reaction of 3,3',4,4'-biphenyltetracarboxylic dianhydride (BPDA) with hexamethylenediamine (HMDA) and 4,4'-oxydianiline (ODA) at stoichiometric dianhydride/diamine ratio of 100:30:70 in N-methyl-2-pyrrolidinone (NMP) solutions by using solution condensation polymerization at room temperature and further imidization at 250°C. The photoinitiator and photo precursor were bis(2,4,6-trimethyl benzoyl) phenylphosphine oxide (Irgacure-819) and 2-hydroxyethyl methacrylate (HEMA), respectively. In this study, we used photosensitive polyimide for insulation layer that created as cover film with the thickness of cover film approximately controlled at 12.5 micron, thus the thickness of cover film was called, as “Ultra-thick” and the area opening of NPSPI films are 4 mm<sup>2</sup> was prepared. The silica domains are responsible for reducing the volume shrinkage of NPSPI films after the curing process by synthesis of negative photosensitive polyimide/silica (POSS) hybrid films. The synthesized NPSPI and NPSPI/silica hybrid films were characterized by FTIR and <sup>1</sup>H-NMR while their morphologies were evaluated by Optical and Confocal Microscope. The thermal stability of the polyimide films was analyzed by TGA and their dielectric constants were confirmed by LCR meter. These results indicated that the prepared NPSPI/silica hybrid films would have the high potential for applications in electrical devices.

Department .....Chemical Engineering..... Student's Signature.....  
Field of Study .....Chemical Engineering..... Advisor's Signature.....  
Academic Year .....2012.....

## ACKNOWLEDGEMENTS

I would like to express my deeply appreciation to my advisor, Associate Professor Dr. M.L. Supakanok Thongyai, Ph.D. to his continuous guidance, enormous number of invaluable discussions, helpful suggestions, warm encouragement and patience to correct my writing. I am thankful to Professor Piyasan Praserttham, Dr.Eng., Assistant Professor Sirirat Wacharawichanant, D.Eng., Assistant Professor Soorathep Kheawhom, Ph.D. and Assistant Professor Anongnat Somwangthanaroj, Ph.D. for serving as chairman and thesis committees, respectively, whose comments were creatively and especially gainful.

Sincere thanks are made to Mektec Manufacturing Corporation (Thailand) Ltd. for supporting the scholarship, the materials for synthesis negative photosensitive polyimide and providing the characterize equipments. Thanks to the learning and working place support from the graduate school at Chulalongkorn University, and Department of Chemical Engineering, Faculty of Engineering Chulalongkorn University.

Sincere thanks to all my friends and all members of the Center of Excellent on Catalysis & Catalytic Reaction Engineering, Department of Chemical Engineering, Chulalongkorn University for their assistance and chummy encouragement.

Finally, I wish to consecrate this thesis to my parents and my families, who generous supported and encouraged me through the year spent on this study.

# CONTENTS

	<b>Page</b>
<b>ABSTRACT (IN THAI)</b> .....	iv
<b>ABSTRACT (IN ENGLISH)</b> .....	v
<b>ACKNOWLEDGEMENTS</b> .....	vi
<b>CONTENTS</b> .....	vii
<b>LIST OF TABLES</b> .....	x
<b>LIST OF FIGURES</b> .....	xi
<b>CHAPTER I INTRODUCTION</b> .....	1
1.1 General introduction .....	1
1.2 The objectives of this research.....	3
1.3 The scope of this research.....	3
<b>CHAPTER II THEORIES</b> .....	4
2.1 Polyimides.....	4
2.1.1 One-step method polymerization .....	5
2.1.2 Two-step method polymerization via poly(amic acids).....	7
2.2 Properties of polyimide films.....	9
2.3 Photosensitive Polyimides .....	13
2.3.1 Types of photosensitive polyimide .....	15
2.3.2 Negative photosensitive polyimide precursors .....	16
2.3.3 Photo-initiator .....	17
<b>CHAPTER III LITERATURE REVIEWS</b> .....	20
<b>CHAPTER IV EXPERIMENTS</b> .....	25
4.1 Materials and Chemicals.....	25
4.2 Synthesis of the negative photosensitive polyimide .....	28
4.2.1 Preparation of the negative photosensitive poly (amic acid) .....	28
4.2.2 Preparation of the negative photosensitive poly (amic acid) incorporate with click chemistry.....	28

	<b>Page</b>
4.2.3 Patterning of the negative photosensitive polyimide .....	28
4.3 Equipment .....	31
4.3.1 Glove box .....	31
4.3.2 Vacuum oven .....	31
4.3.3 UV lamp .....	32
4.3.4 Magnetic stirrer and hot plate .....	32
4.3.5 Laboratory bottles, Syringe, Needle and Glass Substrate .....	33
4.3.6 Transparent mask .....	33
4.4 Characterization Instruments .....	34
4.4.1 Fourier transform infrared spectroscopy (FTIR) .....	34
4.4.2 Nuclear magnetic resonance spectroscopy ( <sup>1</sup> H-NMR) .....	34
4.4.3 Thermogravimetric analysis (TGA) .....	35
4.4.4 LCR meter .....	35
4.4.5 Tensile testing machine .....	36
4.4.6 Confocal microscope .....	36
4.4.7 Optical microscope .....	37
4.4.8 Stylus profiler .....	37
4.4.9 Micrometer .....	38
4.5 Benefits of this research .....	38
4.6 Research methodology .....	39
<b>CHAPTER V RESULTS AND DISCUSSION .....</b>	<b>40</b>
5.1 Negative photosensitive polyimide (NPSPI) and negative photosensitive polyimide/silica (POSS) hybrid materials synthesis .....	40
5.1.1 Preparation of the negative photosensitive polyimide and negative photosensitive polyimide/silica (POSS) hybrid materials synthesis .....	40
5.1.2 Function of the components .....	41



	<b>Page</b>
5.1.3 FTIR spectrum of PI, NPSPI and NPSPI/silica hybrids films	.45
5.1.4 <sup>1</sup> H-NMR of 4-aminobenzenethiol, Octavinyl POSS and 4-aminobenzenethiol incorporated with Octavinyl POSS	.....47
5.2 Determination the thickness of the negative photosensitive polyimide films	.....49
5.3 The effect of developing time on the dissolution in the developer of the negative photosensitive polyimide films	.....50
5.4 Determination of the relation between area openings of negative photosensitive polyimide films with photo-mask size	.....52
5.5 Thermal properties	.....56
5.6 Dielectric properties	.....57
5.7 Tensile properties	.....59
5.8 Volume shrinkage of films	.....60
5.9 Morphology of negative photosensitive polyimide films	.....62
<b>CHAPTER VI CONCLUSIONS AND RECOMMENDATIONS</b>	<b>.....64</b>
6.1 Conclusions	.....64
6.1.1 Synthesis of the negative photosensitive polyimide and negative photosensitive polyimide/silica (POSS) hybrid materials	.....64
6.2 Recommendations	.....65
<b>REFERENCES</b>	<b>.....66</b>
<b>APPENDICES</b>	<b>.....70</b>
APPENDIX A	.....71
APPENDIX B	.....74
APPENDIX C	.....76
<b>VITA</b>	<b>.....78</b>

## LIST OF TABLES

	<b>Page</b>
Table 2.1	Properties of Kapton <sup>®</sup> type H. Typical values (25 $\mu\text{m}$ film) ..... 11
Table 2.2	Properties of Upilex <sup>®</sup> films (25 $\mu\text{m}$ )..... 12
Table 2.3	Process for photolithographic production of highly heat-resistant relief patterns ..... 13
Table 4.1	Chemical structures of materials used in this research ..... 26
Table 5.1	The wave number ratio of (1100/1500) of PI, NPSPI and NPSPI/silica hybrids ..... 46
Table 5.2	Thickness of PI and NPSPI films ..... 49
Table 5.3	Thickness of NPSPI films at various sizes of substrate..... 50
Table 5.4	The thickness of NPSPI films and % dissolution at various developing time..... 51
Table 5.5	The ratio area opening of NPSPI films with photo-mask size 5x5 mm ..... 53
Table 5.6	The ratio area opening of NPSPI films with photo-mask size 4x4 mm ..... 53
Table 5.7	The ratio area opening of NPSPI films with photo-mask size 3x3 mm ..... 54
Table 5.8	The ratio area opening of NPSPI films with photo-mask size 2x2 mm ..... 54
Table 5.9	The ratio area opening of NPSPI/silica hybrid films with photo-mask size 2x2 mm ..... 55
Table 5.10	The degradation temperature of prepared films after curing at 250 $^{\circ}\text{C}$ ..... 56
Table 5.11	Dielectric constant of polyimide films each system ..... 58
Table 5.12	Tensile properties of PI, NPSPI and NPSPI/silica hybrid films ..... 59
Table 5.13	The volume shrinkage of prepared films after curing at 250 $^{\circ}\text{C}$ ..... 60

## LIST OF FIGURES

		<b>Page</b>
Figure 2.1	Structure of an imide group .....	4
Figure 2.2	Structure of types of polyimide.....	4
Figure 2.3	Aromatic polyimides repeating unit.....	5
Figure 2.4	Reaction of dicyanomethylidene phthalide with aniline.....	6
Figure 2.5	Polymerization of bisdicyanomethylidene derivative of PMDA with ODA.....	6
Figure 2.6	Reaction for the preparation of Kapton™ polyimide .....	7
Figure 2.7	Reaction mechanism of imide formation.....	8
Figure 2.8	Commonly used dianhydride monomers. ....	9
Figure 2.9	Commonly used diamine monomers .....	9
Figure 2.10	Process simplification opportunity using photosensitive polyimide as compared with conventional nonphotosensitive polyimide .....	14
Figure 2.11	The principle of positive and negative photosensitive polyimide processing .....	15
Figure 2.12	The ring closure reaction .....	17
Figure 2.13	The wavelength range of IRGACURE 819 is absorbed .....	19
Figure 2.14	Thermal stability of the individual IRGACURE photo-initiator .....	19
Figure 4.1	Preparation of negative photosensitive poly (amic acid).....	29
Figure 4.2	Preparation of negative photosensitive poly (amic acid)/silica hybrids.....	30
Figure 4.3	Glove box.....	31
Figure 4.4	Vacuum oven .....	31
Figure 4.5	UV lamp.....	32
Figure 4.6	UV meter.....	32
Figure 4.7	Transparent mask .....	33
Figure 4.8	Fourier transform infrared spectroscopy (FTIR) Equipment .....	34

	<b>Page</b>
Figure 4.9	Nuclear magnetic resonance spectroscopy (NMR) Equipment.....34
Figure 4.10	Thermogravimetric analysis (TGA) Equipment.....35
Figure 4.11	LCR meter Equipment.....35
Figure 4.12	Tensile testing machine Equipment.....36
Figure 4.13	Confocal microscope Equipment .....36
Figure 4.14	Optical microscope Equipment .....37
Figure 4.15	Stylus profiler Equipment.....37
Figure 4.16	Micrometer Equipment.....38
Figure 4.17	Flow diagram of research methodology .....39
Figure 5.1	Preparing negative photosensitive poly (amic acid) .....43
Figure 5.2	Preparing negative photosensitive poly (amic acid)/silica hybrids.....44
Figure 5.3	FTIR spectra of prepared films, PI, NPSPI and NPSPI/silica hybrids 46
Figure 5.4	<sup>1</sup> H-NMR of 4-aminobenzenethiol.....47
Figure 5.5	<sup>1</sup> H-NMR of Octavinyl POSS .....47
Figure 5.6	<sup>1</sup> H-NMR of 4-aminobenzenethiol incorporated with Octavinyl POSS .....48
Figure 5.7	The relation between % dissolution of the exposed and unexposed areas of polyimide films in the developing solvent with each developing time.....52
Figure 5.8	Position of the area opening of NPSPI films with photo-mask size 5x5 mm .....53
Figure 5.9	Position of the area opening of NPSPI films with photo-mask size 4x4 mm .....53
Figure 5.10	Position of the area opening of NPSPI films with photo-mask size 3x3 mm .....54
Figure 5.11	Position of the area opening of NPSPI films with photo-mask size 2x2 mm .....55

	<b>Page</b>
Figure 5.12	Position of the area opening of NPSPI/silica hybrid films with photo-mask size 2x2 mm .....55
Figure 5.13	The relation between % weights of polyimide films with temperature .....57
Figure 5.14	Tensile strengths of PI, NPSPI and NPSPI/silica hybrid films.....59
Figure 5.15	Thickness variations of PI, NPSPI and NPSPI/silica hybrid films in the curing process .....61
Figure 5.16	Photograph of NPSPI films (a) from Mobile phone (b) from Optical microscope .....62
Figure 5.17	Morphology of NPSPI films on copper foil. [Size of opening of 2x2 mm] .....62
Figure A-1	Stylus profiler diagrams of NPSPI films with photo-mask size 2x2 mm at position (a) .....71
Figure A-2	Stylus profiler diagrams of NPSPI films with photo-mask size 2x2 mm at position (b).....72
Figure A-3	Stylus profiler diagrams of NPSPI films with photo-mask size 2x2 mm at position (c) .....72
Figure A-4	Stylus profiler diagrams of NPSPI films with photo-mask size 2x2 mm at position (d).....73
Figure B-1	Thermogravimetric analysis of PI films at rate 10°C/min, in N <sub>2</sub> .....74
Figure B-2	Thermogravimetric analysis of NPSPI films at rate 10°C/min, in N <sub>2</sub> .75
Figure B-3	Thermogravimetric analysis of NPSPI/silica hybrids films at rate 10°C/min, in N <sub>2</sub> .....75
Figure C-1	Tensile strengths of PI films at 5.76% of tensile strain at break.....76
Figure C-2	Tensile strengths of NPSPI films at 6.25% of tensile strain at break ..77
Figure C-3	Tensile strengths of NPSPI/silica hybrids films at 2.61% of tensile strain at break .....77

# CHAPTER I

## INTRODUCTION

### 1.1 General introduction

Polyimides (PIs) are outstanding polymers which have many uses in microelectronics and aerospace industry, such as high temperature insulators, dielectrics, coatings, adhesives and advanced composite matrices because of their thermal stability, excellent chemical resistance, and good electrical and mechanical properties. [1] In addition, polyimides are strongly absorbed visible light with wavelength in the range about 400-700 nm and have relatively high dielectric constants over 3.0. [2,3]

Polyimides or non-photosensitive polyimide can only be applied as total cover film (cannot be directly patterned) and requires several process steps after the active device was created. On the other hand, photosensitive polyimides can be directly patterned and processed similar to standard resistors using photolithography techniques. An eight-step conventional polyimide process can be consolidated into a three-step process using photosensitive polyimide. [4] The resulting was time saving and cost reduction of production. Therefore, photosensitive polyimides (PSPIs) have attracted a great interest nowadays. Typically, photosensitive polyimide practiced for an insulation layer film in semiconductor microelectronic industry has the thickness of the film at approximately 5 micron. In this project, we used photosensitive polyimide for insulation created as cover film so the thickness of cover film should be enlarged from 5 micron to about 12.5 micron. We call this thickness of cover film as “Ultra-thick”. The opening size of cover film is larger than 2 mm so the correlation of opening area and mask size was investigated in this research.

Photosensitive polyimide can be categorized into two types, negative and positive photosensitive polyimide. Positive photosensitive polyimide has limited applications in usage because of the narrow available film thickness range. Negative photosensitive polyimide is available in a wide range of viscosities. [5] Mainly, negative photosensitive polyimide is usually used for photosensitive polyimide systems.

The applications of photosensitive polyimides on optoelectronic devices are importantly limited because large volume shrinkage after curing (often up to 20–50%) because of elimination of pendant photosensitive moieties during curing process. Such large volume shrinkage would cause a significant distortion of the patterned feature. [6] Hence, the reduction of volume shrinkage for photosensitive polyimide has become the major interest. The approach of preparing photosensitive polyimide/silica hybrid materials could resolve the above problems of photosensitive polyimide materials for optoelectronic devices [7-11]. Many successful attempt of silica hybrid can reduce the shrinkage of photosensitive polyimide up to around 6-8 percent [13,29-30] However, the usage of POSS (Polyhedral Silsesquioxane) as the effective silica hybrid for the purpose has never been investigated before, so this is the main theme of the research.

In this study, synthesis of negative photosensitive polyimide incorporated with silica (POSS) at end of molecule of polyimide was investigated in order to reduce the volume shrinkage. Thus, the target of producing ultra-thick negative photosensitive polyimide with less volume shrinkage is worth investigation.

## **1.2 The objectives of this research**

1.2.1 To synthesize ultra-thick (more than 12.5 micron) negative photosensitive polyimide (NPSPI).

1.2.2 To synthesize ultra-thick negative photosensitive polyimide/silica (POSS) hybrid materials with less shrinkage after cured.

1.2.3 To determine the thickness (about 12.5 micron) and the relation between opening size of negative photosensitive polyimide films and photo-mask size. (To obtain the opening ratio)

1.2.4 To improve thermal and mechanical properties of negative photosensitive polyimide films for patterned electronic devices.

## **1.3 The scope of this research**

1.3.1 Synthesize polyimide from 3,3',4,4'-biphenyltetracarboxylic dianhydride (BPDA) with hexamethylenediamine (HMDA) and 4,4'-oxydianiline (ODA).

1.3.2 Synthesize negative photosensitive polyimide based on 2-hydroxyethyl methacrylate (HEMA) photosensitive precursor and Bis(2,4,6-trimethylbenzoyl)phenyl phosphine oxide (Irgacure-819) photosensitive initiator.

1.3.3 Synthesize negative photosensitive polyimide/silica (POSS) hybrid materials by incorporating click chemistry based on 4-Aminobenzenethiol and Octavinyl POSS at end molecule of polyimide.

1.3.4 Measure the thickness and ratio of opening size between opening area of ultra-thick (12.5 Micron) NPSPI films to area of photo-mask when the thickness and opening size of NPSPI films are larger than 12.5 micron and 2x2 mm, respectively.

1.3.5 Characterize negative photosensitive polyimide and negative photosensitive polyimide polyimide/silica (POSS) hybrid materials properties by conventional techniques: FTIR, <sup>1</sup>H-NMR, TGA, LCR meter, tensile testing machine, confocal microscope, optical microscope and stylus profiler.



## CHAPTER II

### THEORIES

This chapter describes the main details of the basic theories about polyimides, properties of polyimide films and photosensitive polyimides, explained in section 2.1, 2.2 and 2.3, respectively.

#### 2.1 Polyimides

Polyimides are commonly used in many electronic applications because of their high performance such as high thermal stability, good chemical resistance, excellent mechanical and electrical properties [7-12]. Polyimides are polymers of imide monomers. An imide is a group of bonds in a molecule that has a general structure as shown in Figure 2.1. Commonly, polyimides get one of two forms, the first of these structures is a linear structure which the atoms of the imide group are section of a linear chain and the second of these structures is a heterocyclic structure which the imide group is a section of a cyclic unit in the polymer chain as shown in Figure 2.2

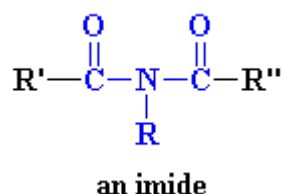


**Figure 2.1** Structure of an imide group [13]

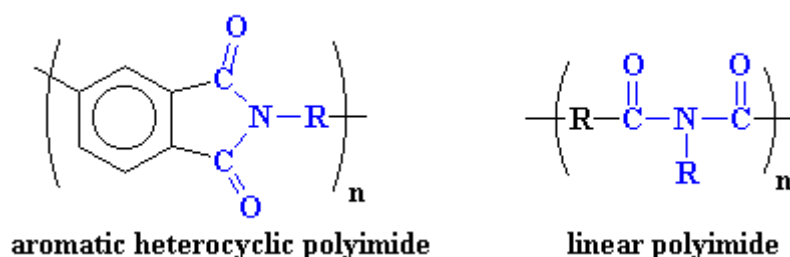


**Figure 2.2** Structure of types of polyimide [13]

Polyimides are polymers formed by the condensation reactions of dianhydrides and diamines. The structure of polyimide that has been synthesized from aromatic dianhydrides and aromatic diamines or from aromatic dianhydrides and aliphatic diamines can be shown in Figure 2.3. Aromatic polyimides are often infusible and insoluble so precipitation occurs during the intermediate stages of polymerization. The condensation is accomplished in two stages. First, a noncyclized polymer (polyamic acids) is generated by a rapid reaction in a polar solvent at temperature below 70 °C. Second, a noncyclized polymer, polyamic acid, can be fabricated to an appropriate shape and then cyclized to polyimides by heating at temperature up to 300 °C. Such polymers are rigid, have high melting point and are thermally stable [14].

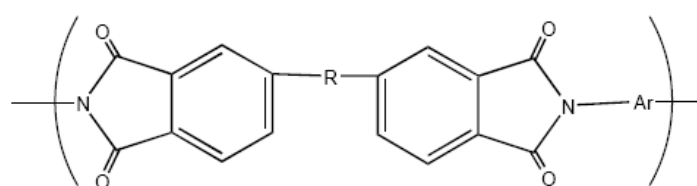


**Figure 2.3** Aromatic polyimides repeating unit [15]

There are two methods to synthesize polyimides, one-step and two-step methods. The details for synthesis of polyimides are as follows.

### 2.1.1 One-step method polymerization

#### 1) High-temperature solution polymerization

This method is used for polyimides that are soluble in organic solvents at polymerization temperatures [15]. The process involves a mixture of solvents or heating a stoichiometric mixture of monomers in a high boiling point solvent at a temperature range of 180°C-220°C [16] where the imidization reaction proceeds rapidly and, during polymerization, water is distilled off continuously as an azeotrope with toluene along with the solvent. The generally utilized solvents are nitrobenzene, m-cresol and dipolar aprotic amide solvents. Furthermore, toluene is frequently used as a cosolvent to enable the removal of the water in condensation by azeotropic

distillation. The imidization still proceeds via the amic acid route although the concentration of amic acid at any time is very small because it is unstable at high temperature so the amic acid group rapidly converts to an imide or reverts back to amine and anhydride. For polymerization, quinoline, tertiary amines, alkali metals and zinc salts are often accomplished in the presence of catalysts of carboxylic acids at the high temperature solution [17]. This process is especially useful for polymerization involving unreactive dianhydrides and diamines. An interesting feature of this method is that it often yields materials with a higher degree of crystallinity than the material from two-step methods [18], which may be due to the increased solubility of the monomers in the solvent medium.

## 2) Low-temperature solution polymerization

Another way for one-step method polymerization is low-temperature solution polymerization. Kim and Moore [18] synthesized a dicyanomethylidene derivative of phthalic anhydride as illustrated in Figure 2.4. The model compound reacted versus aniline in NMP solvent to produce an intermediate of amic acid analog that slowly converted at room temperature during 24 h to *N*-phenylphthalimide, co-producing malonitrile as condensation by product. Furthermore, bis(dicyanomethylidene) derivative of PMDA and ODA were reacted in NMP solvent to provide poly(amic acid) analog intermediate, which at room temperature underwent partial imidization in the homogeneous solution, as displayed in Figure 2.5.

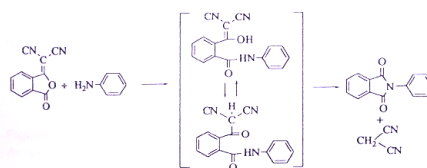


**Figure 2.4** Reaction of dicyanomethylidene phthalide with aniline [13]

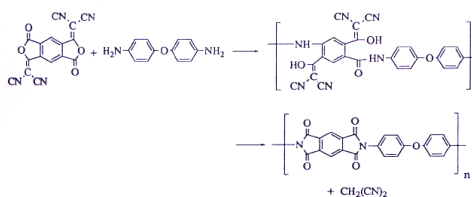


**Figure 2.5** Polymerization of bisdicyanomethylidene derivative of PMDA with ODA [13]

The imidization achieved about 75% over 24 h, after the time, which the polymer began to precipitate. The solid-state imidization of films prepared from the poly(amic acid) analog intermediate acted likewise to that of poly(amic acid) nevertheless, the imidization could be reached at lower temperature; it was almost completed in 20 h at 120 °C.

### 2.1.2 Two-step method polymerization via poly(amic acids)

This method is the most widely practiced procedure in polyimide synthesis. In this process, a dianhydride and a diamine react at ambient conditions in a dipolar aprotic solvent such as *N,N*-dimethylacetamide (DMAc) or *N*-methylpyrrolidinone (NMP) to yield the corresponding poly(amic acid), which is then cyclized into the polyimide. The earlier originators at DuPont Co. coped with this common method. The majorities of polyimides are infusible and insoluble because their planar aromatic and heteroaromatic structures so they usually need to be processed from the solvent route. This method provided the first method of such solvent based route to process these polyimides. The process also enabled the first polyimide of significant commercial importance ‘Kapton™’ to enter the market. Figure 2.6 presents an example of the synthesis for Kapton polyimide utilizes the monomer pyromellitic dianhydride (PMDA) and 4,4'-oxydianiline (ODA).

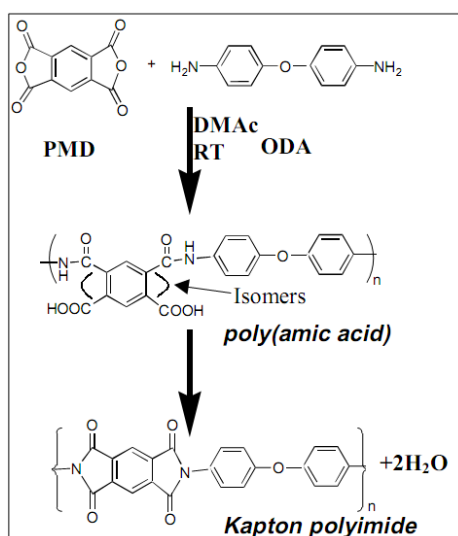


**Figure 2.6** Reaction for the preparation of Kapton™ polyimide [16]

Poly(amic acid)s can be formed into sections such as films and fibers by removal of solvent. The formed poly(amic acid) films, such as, are further thermally or chemically converted to the final polyimide products. When a diamine and a dianhydride are added into a dipolar aprotic solvent such as DMAc or NMP, then poly(amic acid) is rapidly formed at room temperatures due to nucleophilic attack of the amino group on the carbonyl carbon of the anhydride group, followed by the opening of the anhydride ring to form amic acid group [19]. After that poly(amic acid)s are heated gradually up to 250-350°C (imidization), depending upon the stability and glass transition temperature ( $T_g$ ) of the polymer therefore poly(amic acid)s becomes polyimides. The conversion produces water as a by-product, therefore water must be removed during this in-situ imidization. The reaction mechanism is represented in Figure 2.7. The process is generally suitable only for the preparation of thin object such as films because of the difficulty to remove water from the reaction.

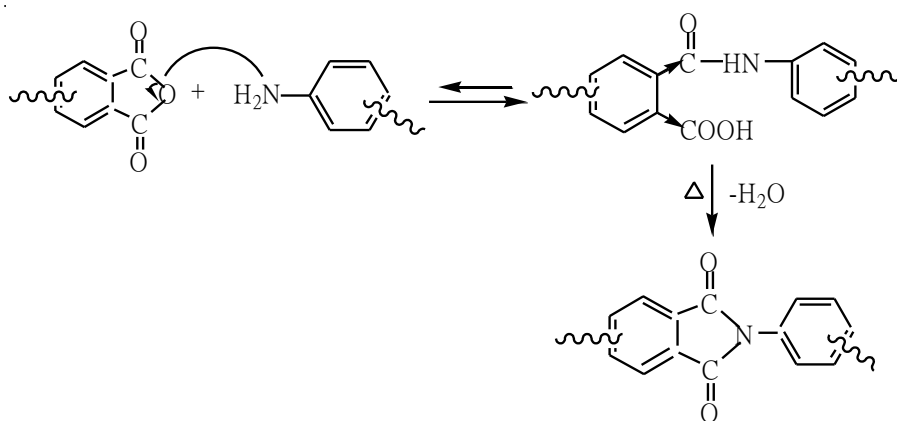


**Figure 2.7** Reaction mechanism of imide formation [13]

Polyimide involves reacting of a dianhydride and a diamine monomer. Commonly used dianhydride and diamine monomers are shown schematically in Figure 2.7 and 2.8, respectively.

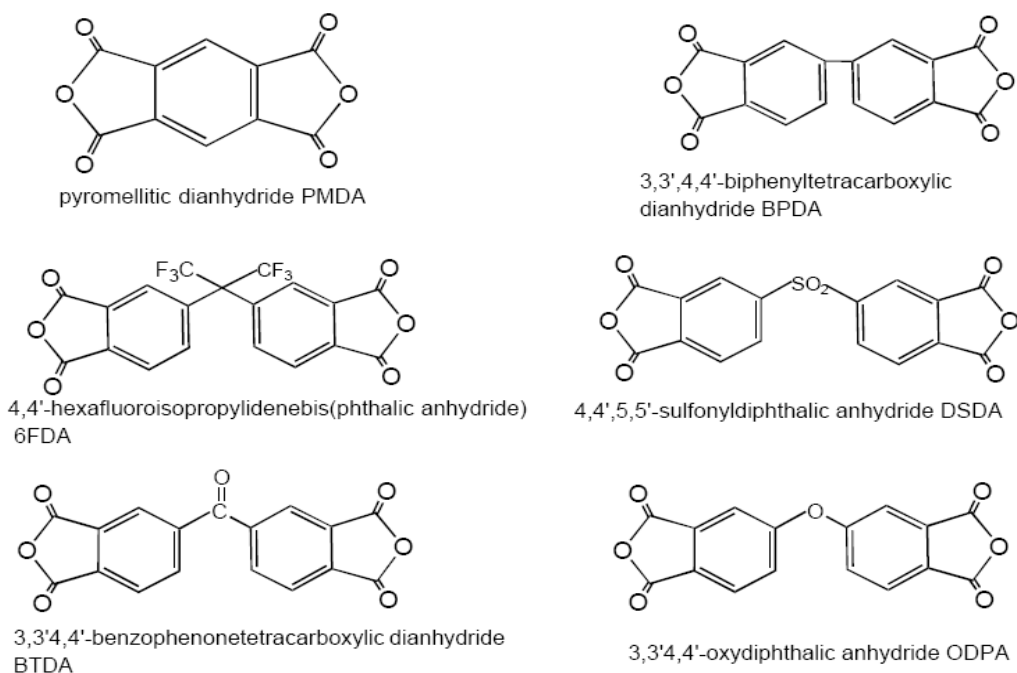


**Figure 2.8** Commonly used dianhydride monomers [20]

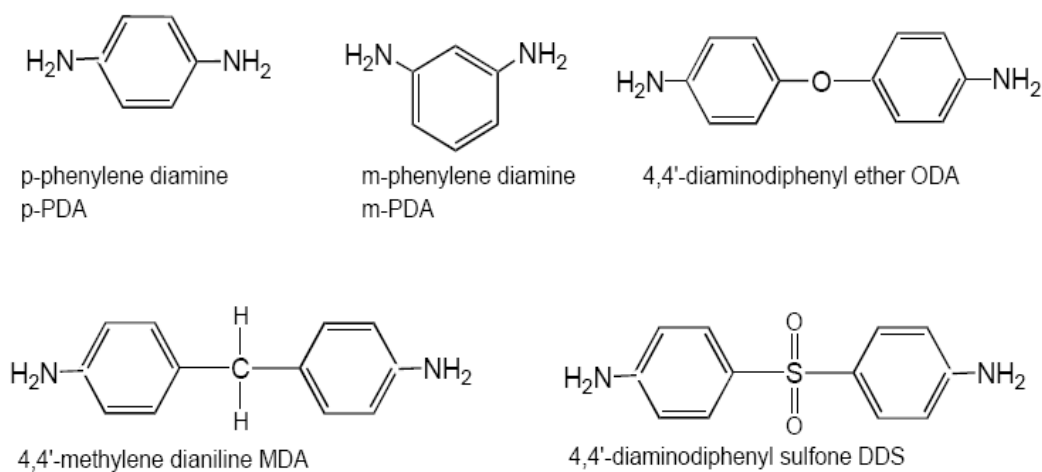


**Figure 2.9** Commonly used diamine monomers [20]

## 2.2 Properties of polyimide films

Aromatic polyimides films evince the largest end-use area for the polyimides. Films of polyimide are prepared with casting solutions of poly(amic-acid) precursor onto a substrate and transforming to the polyimide film then conversion can be completed chemically or thermally by heating to temperature over 300°C.

Polyimides have been accepted from the earliest days of their fabrication for their excellent thermal stability. Beyond thermal endurance, the preliminary references to polyimide films explained and italicized the width of valuable properties above more broad temperature range. Du Pont's Kapton<sup>®</sup> was recognized standard of superiority for many years and then Kapton<sup>®</sup>'s properties are concluded in Table 2.1. Ube's films out of BPDA are marketed by ICI under the trade name Upilex<sup>®</sup>. Upilex R<sup>®</sup> is the polyimide out of ODA-BPDA, and then Upilex S<sup>®</sup> is the polyimide out of PPD-BPDA. Properties for these films are concluded in Table 2.2.

The comparison of Kapton<sup>®</sup> versus the Upilex<sup>®</sup> films is recommend structurally and important in terms of gainful properties. Upilex R<sup>®</sup> is preferable in lower H<sub>2</sub>O regain, lower shrinkage at 250 °C, and excellent hydrolytic resistance, especially to aqueous NaOH. Upilex R<sup>®</sup>, carrying the like diamine as Kapton<sup>®</sup>, has an essentially lower T<sub>g</sub>, however, is comparative to Kapton<sup>®</sup> in electrical and mechanical properties both at room and at high temperatures. Upilex S<sup>®</sup> is essentially different from Kapton<sup>®</sup>. It is very hard, has much lower % elongation with resulting potential for brittleness, has higher tensile strength, significantly lower high temperature shrinkage, and lower thermal and hygroscopic coefficients of expansion. For many microelectronic and aerospace industries that Kapton<sup>®</sup> has showed a major role in aerospace wire and cable, magnet wire, flexible printed circuits, capacitors, transformers and many other uses. In recent years, the electronic circuitry has become more essential with increasing polyimide use not only as film base however also in laminates, particularly with copper. Upilex S<sup>®</sup> presents to prefer significant potential competition to Kapton<sup>®</sup> because it is specifically in circuitry applications. [21]

**Table 2.1** Properties of Kapton<sup>®</sup> type H. Typical values (25  $\mu\text{m}$  film) [21]

Property	-195 °C	25 °C	200 °C
<b>Physical Properties</b>			
Tensile strength, MPa	241	172	117
Stress at 5% elongation, MPa	-	90	55
Ultimate elongation %	2	70	90
Tensile modulus, GPa	3.5	3.0	1.8
Folding endurance (MIT)	-	10000 cycles	-
Tear strength - propagating (Elmendorf) kg/mm	-	0.32	-
Tear strength – initial (Graves) kg/mm	-	20.1	-
Density g/cm <sup>3</sup>	-	1.42	-
<b>Thermal Properties</b>			
Glass transition temperature		385 °C	
Cut-through temperature		435 °C (25 $\mu\text{m}$ ); 525 °C (50-125 $\mu\text{m}$ )	
Coefficient of thermal expansion		2.0 x 10 <sup>-5</sup> m/m/°C	
Heat aging in air		250°C (8 years); 275°C (1 year) 300°C (3 months ; 400°C (12 hr)	
Shrinkage % (250°C /30min)		0.3%	
Oxygen index (%)		37	
<b>Electrical Properties</b>			
Dielectric strength (25 $\mu\text{m}$ )volts	10000	7000	5600
Dielectric constant (10 <sup>3</sup> Hz)	-	3.5	3.0
Dissipation factor (10 <sup>3</sup> Hz)	-	0.003	0.002
Volume resistivity (at 50% RH)	-	10 <sup>18</sup> ohm-cm	10 <sup>14</sup> ohm-cm
Corona start voltage (at 50% RH)	-	465 volts	-
Surface resistivity	-	10 <sup>16</sup> ohm	
<b>Chemical Properties</b>			
Hygroscopic coefficient of Expansion		2.2 x 10 <sup>-5</sup> m/m/% RH (72°F 20-80% RH)	
Moisture absorption		1.3% (50% RH (23.5°C) 2.9% (immersion 24 hr/23.5°C)	
gas permeability (l/m <sup>2</sup> /day/(MPa/mm)): 23°C			
He	1.61		
CO <sub>2</sub>	0.174		
H <sub>2</sub>	0.97		
N <sub>2</sub>	0.023		
O <sub>2</sub>	0.097		
H <sub>2</sub> O vapor (kg/m <sup>2</sup> /day/(MPa/mm))	0.021		
Solvent resistance		excellent	



**Table 2.2** Properties of Upilex<sup>®</sup> films (25  $\mu$ m) [21]

	Upilex R (from ODA)	Upilex S (from PPD)
<b>Mechanical Properties</b>		
23°C		
Tensile strength(MPa)	172	276
Stress at 5% E (MPa)	83	180
Elongation (%)	130	30
Tensile modulus (GPa)	2.6	6.2
200°C		
Tensile strength (MPa)	138	151 (300°C)
Stress at 5% E (MPa)	41	62
Elongation (%)	130	30
Tensile modulus (GPa)	1.4	6.2
Tear strength (23°C) Elmendorf	0.75	0.30
Propagation kg/m		
MIT fold	>10 <sup>5</sup>	>10 <sup>5</sup>
Density (g/cm <sup>3</sup> )	1.38	1.47
<b>Electrical properties</b>		
25°C		
Volume resistivity (ohm-cm)	10 <sup>17</sup>	10 <sup>17</sup>
Dielectric constant (10 <sup>3</sup> HZ)	3.5	3.5
Dissipation factor (10 <sup>3</sup> HZ)	0.0014	0.0013
Dielectric strength (kV/mm)	280	286
200°C		
Volume resistivity (ohm-cm)	10 <sup>15</sup>	10 <sup>15</sup>
Dielectric constant (10 <sup>3</sup> HZ)	3.2	3.3
Dissipation factor (10 <sup>3</sup> HZ)	0.0040	0.0078
Dielectric strength (kV/mm)	280	270
<b>Thermal properties</b>		
Thermal coefficient of expansion	1.5 (MD)	0.8 (MD) (20-100c;cm/cm/°C x10 <sup>-5</sup> )
Shrinkage (%) (250°C /2 hr)	0.18	0.07
Glass transition temperature	285°C	>500°C
Oxygen index (%)	55	66
Solvent sensitivity	Low	Low
Hygrosopic coefficient expansion (cm/cm/%RH)20-80% RH x 10 <sup>-5</sup> )	2	1
<b>Chemical Properties</b>		
Gas Permeability	0.56	0.043
20°C /24 hr water vapor (g/m <sup>2</sup> /mm)		
30°C (ml/m <sup>2</sup> /mm)		
Oxygen	2.54	0.02
Nitrogen	0.76	-
Carbon dioxide	2.92	0.030
Helium	55.9	-
60% H <sub>2</sub> O regain	1.1	0.9
Solvent Resistivity	Excellent	Excellent

### 2.3 Photosensitive Polyimides

Polyimides have shown an increasing role in electronics for a variety of applications include use as a base sheet film for flexible circuitry, coatings for computer chips, interlayer dielectrics, and, as seen earlier, in circuit boards, cross-linked polyimides have found significant benefit. Increasing integration in solid-state technology has set increasing economic needs on reducing the defect density of the circuits achieved and on speed of creating complex patterned circuitry. A significant response to the increased complexity of circuits and the cost burden of multistep processing has been directly to use photosensitive polyimide precursors. [21]

**Table 2.3** Process for photolithographic production of highly heat-resistant relief patterns [21]

		<b>Polyimide Copolymer Precursor PIQ + Negative Resist</b>	<b>Processing Step</b>	<b>Photo-cross linkable Polyimide</b>
I.	Coupler	Yes	Coating	Not necessary
		Yes	Thermal treatment	Not necessary
II.	Polyimide precursor	Yes	Coating	Yes
		Yes	Thermal Coating	Yes
III.	Photoresist	Yes	Coating	Not necessary
		Yes	Drying	Not necessary
		Yes	Exposing	Yes
		Yes	Developing	Not necessary
		Yes	Developing of Polyimide precursor	Yes
		Yes	Removal of coupler	Not necessary
		Yes	Washing/drying	Not necessary
		Yes	Removal of photoresist	Not necessary
IV.	Polyimide pattern	Yes	Drying thermal treatment	Yes

\*PIQ = Poly-Isoindolo-Quinazolinedione

Table 2.3 shows comparison of the older use of photoresistants to the newer use of photosensitive polyimide precursors. It is obvious that the process using photosensitive polyimides requires fewer operational steps thus decreasing processing

costs. A supplementary essential result is to reduce the number of defects, since each extra processing step suggests its share of defects.

Conventional or nonphotosensitive polyimide cannot be directly patterned and requires several process steps after the active device is created. This technical difficulty combined with the complexity of the process has limited the nonphotosensitive polyimide application. Subsequently, simplified photosensitive polyimide process is offered for a cost savings alternative to the buffer coat polyimide application. Photosensitive polyimides can be processed similar to standard resists using photolithography techniques, which an eight-step conventional polyimide process can be consolidated into a three-step process using photosensitive polyimide. Then a demonstration of this process simplification can be shown in Figure 2.10. [4]

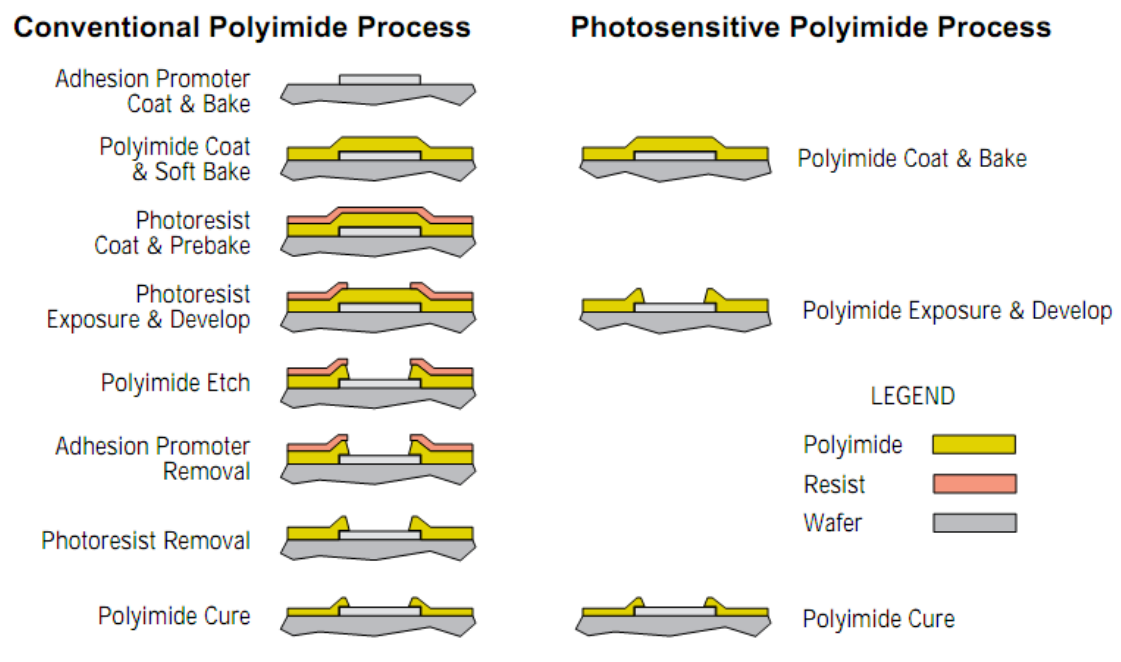


**Figure 2.10** Process simplification opportunity using photosensitive polyimide as compared with conventional nonphotosensitive polyimide. [4]

Polyimide applications in electronics are associated to certain key polyimide properties. These include thermal stability, ability of solution coating of soluble poly(amic acid) precursors, toughness of polyimide film after final curing, excellent dielectric properties, and outstanding dimensional stability of the final converted

polyimide. All of these properties are object to increasing requires for improvement as further demands of circuit reliance and increased pattern density occur. Photosensitive polyimide materials have come to the market from a large number of companies for example Du Pont, Hitachi, Toray, Siemens, Ciba-Geigy, Philips and BASF.

### 2.3.1 Types of photosensitive polyimide

Photosensitive polyimides, like photoresist, can be divided into two major categories; negative or positive tone. Application of positive photosensitive polyimide is limited because of the narrow film thickness range available. Negative photosensitive polyimides are available in a wide range of viscosities. [5] Figure 2.11 shows the basics of photolithography, which the desired pattern is created by irradiating through a mask in order to expose selected regions of the photoresist material. The significant difference between negative and positive photoresists is the way photo react with polyimide. In a negative photoresist, exposure to light renders the photoresists insoluble due to exposure leads to cross-linking, polymer less soluble in the developer. The unexposed regions of the photoresist are removed by the solvent, revealing the substrate below. Since the substrate is actually the key electronic material here (typically silicon or gold, etc.), the process is considered “negative” because the exposed regions of the substrate were not exposed to light. In contrast, exposure of a positive photoresist to light increases its solubility because exposure leads to breaking polymer chains, the polymer dissolves easily in developer. Treatment with solvent reveals those regions of the substrate that were exposed to light.

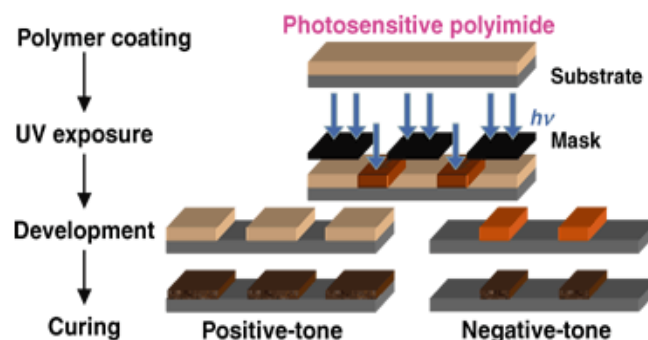


**Figure 2.11** The principle of positive and negative photosensitive polyimide processing. [21]

### 2.3.2 Negative photosensitive polyimide precursors

The polyimide precursor is a polymeric resin that can be cross-linked by initiation step of “free radical” so this cross-linked polymer becomes insoluble. The cross-linked polymer is heated via a molecular in which the cross-linking groups are volatilized and the molecules of polyamic acid ester rearrange to polyimide. Then a reaction of this process is represented in Figure 2.11. This polyimide is essentially a linear or non-cross-linked polymer because its chemistry is insoluble in virtually all solvents. For the reaction of cross-linking polymer, it can be initiated with a photo-initiator. Breaking of a molecule of initiator due to exposure by UV light gives rise to a reactive free radical. These free radicals cause the polyimide precursor to cross-link. In this method, UV light can be used to form an image in the polyimide precursor since it cross-links and becomes insoluble when it has been exposed to light and can be washed away during the development step, when it has not been exposed to light. Photosensitive polyimide systems, which make use of this type of chemistry are ‘negative working systems’ [13]

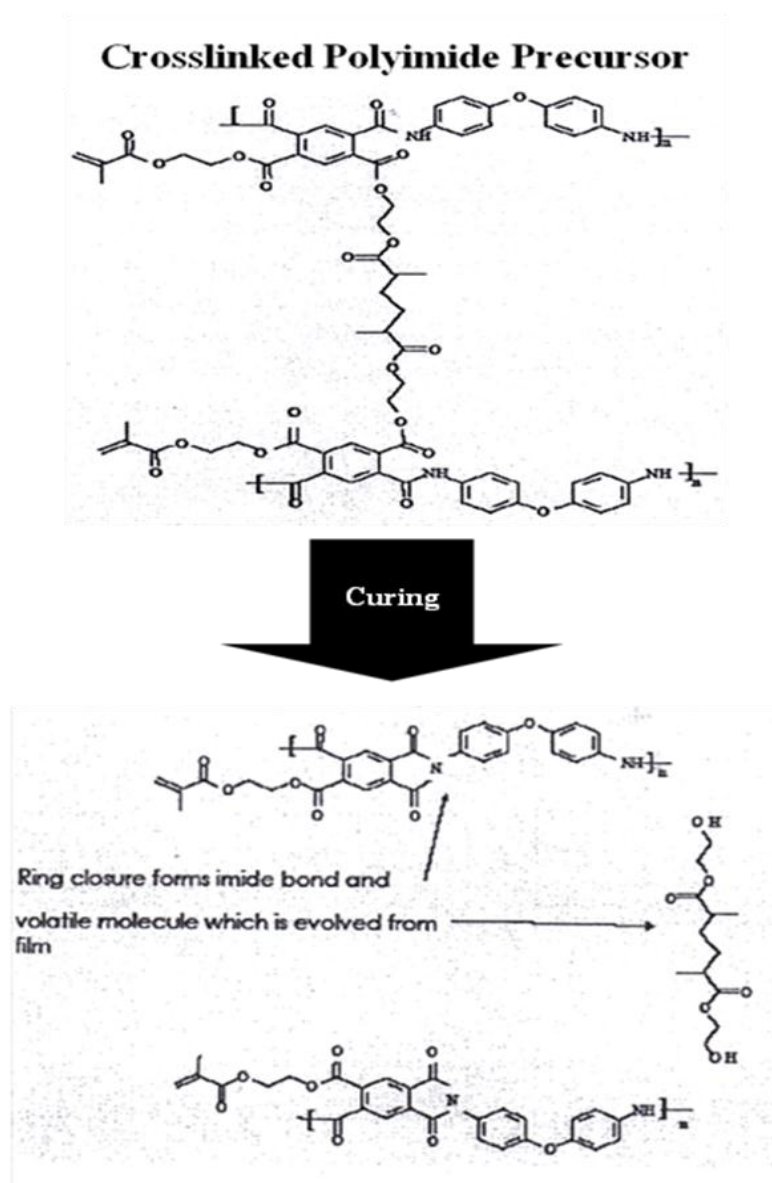


**Figure 2.12** The ring closure reaction [13]

### 2.3.3 Photo-initiator

A photo-initiator is a compound, which, upon absorption of light, undergoes a photoreaction, produces reactive species. The latter are competent of initiating or catalyzing chemical reactions, which result in important changes in the solubility and physical properties of appropriate formulations. Therefore the photo-initiator is a compound transforming the physical energy of light into suitable chemical energy in the form of reactive intermediates. Most commonly, these changes activate polymerization or polycondensation reactions. When initiated with a photo-

initiator and light, this process is called photo polymerization or radiation curing. It transforms a liquid and soluble formulation into a hard and insoluble cross-linked polymer network. Usually, there are two types of photo-initiator that are used in photosensitive polyimides which the details are as follows,

### 1. Radical photo-initiators

Radical photo-initiators are water-compatible and act on molecules containing an acrylate or styrene group has found most widespread application so far and a broad variety of radical photo-initiators have been developed. The range of radiation curing wavelengths used is typically near UV (300-400 nm) but recent progress in initiator chemistry is expanding the ranges of wavelengths that can be used. Ultraviolet light is light that occurs between the visible spectrums and x-rays. Ultraviolet light is light in the wavelength range of 10 nm to 400 nm with energies from 3 eV to 124 eV. For example of photo-initiator, Bis (2,4,6-trimethylbenzoyl) phenyl phosphine oxide or IRGACURE 819 (used in this research) is a multipurpose photo-initiator for radical polymerization of unsaturated resins upon UV light exposure. IRGACURE 819 can easily be used in combinations with UV absorbers due to its photosensitivity at longer wavelengths. It is ideally suited for use in weather-resistant UV curable coatings. The amount of IRGACURE 819 required for optimum performance should be determined in trials covering a concentration range. IRGACURE 819 is especially designed to be activated by longer wavelength UV light in the near visible region above 430 nm. Light of this wavelength penetrates deeper into the lower layers of the coating, so enabling the through curing desired. For shorter wavelength light, around 230 nm, is of higher photon energy but is less penetrating than longer wavelengths. Light of this shorter wavelength is particularly useful for surface curing. From Figure 2.13 present the wavelength range of IRGACURE 819 is absorbed. In addition, thermal stability of IRGACURE 819 after UV exposure is excellent through cure properties that is shown in Figure 2.14

However, selection of the best individual photo-initiator or combination is dependent on a number of variables including chemistry of the resin system (UPES, epoxy acrylate, urethane acrylate), selection of monomers (monofunctional,

multifunctional acrylate monomers), UV lamp type and orientation, cure speed required, coating property requirements, substrate and many others. [22]

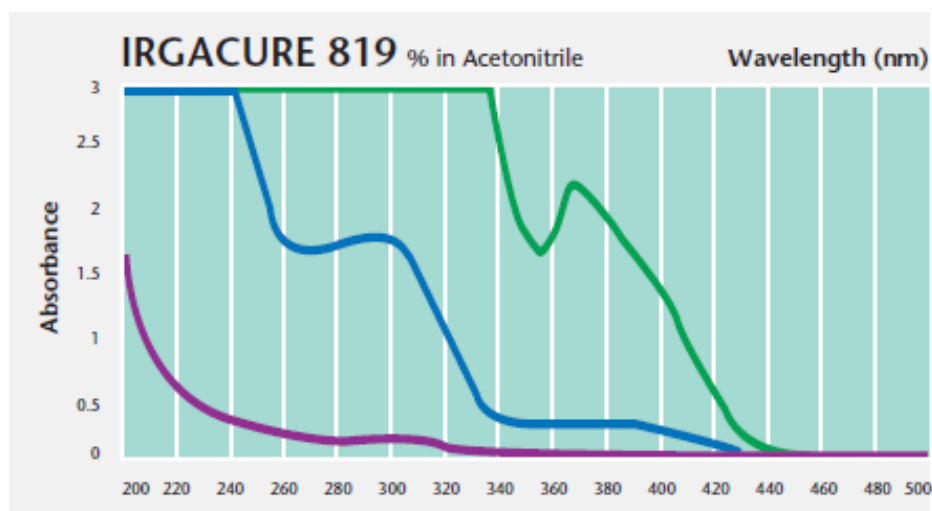


**Figure 2.13** The wavelength range of IRGACURE 819 is absorbed [22]

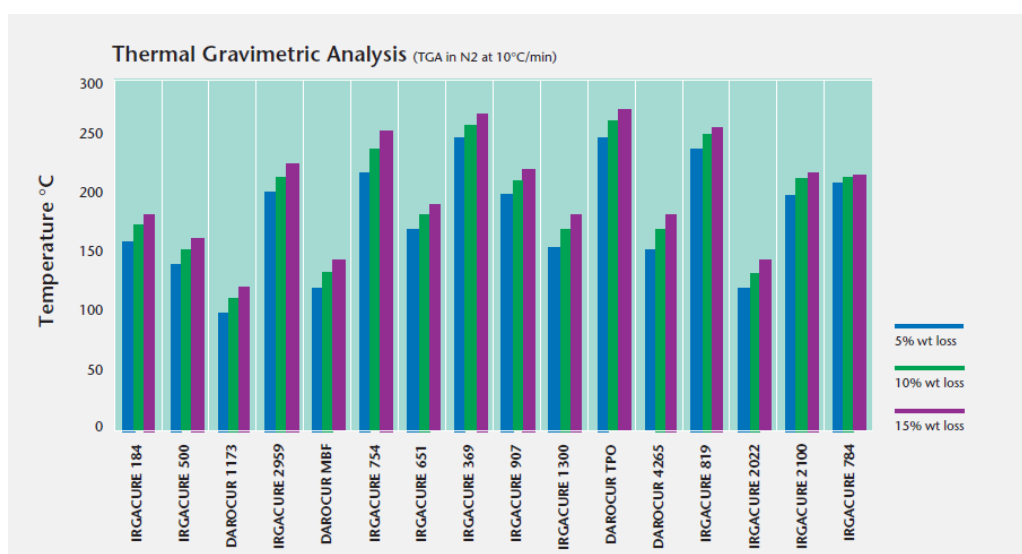


**Figure 2.14** Thermal stability of the individual IRGACURE photo-initiator [22]

## 2. Cationic photo-initiators

Cationic photo-initiators, producing either a Brönsted or Lewis acid, are used as initiators for cationically polymerizing materials (e.g. epoxies) or for resins capable of undergoing cross-linking via polycondensation reactions.



## **CHAPTER III**

### **LITERATURE REVIEWS**

Polyimides have become the standard material that used in a variety of semiconductor manufacturing processes [23] such as buffer coating, passivation layers, alpha particle barrier, interlayer insulation and wafer scale packages, etc. [17] Polyimides are commonly used in many electronic applications because of their high performance such as high thermal stability, good chemical resistance, excellent mechanical and electrical properties. [24] Photosensitive polyimide, like photoresist, can be divided up into two types, negative and positive photosensitive polyimide. Application of positive photosensitive polyimide is limited because of the narrow film thickness range available. Negative photosensitive polyimides are available in a wide range of viscosities [5]. The photosensitive polyimides (PSPIs) simplify the processing steps by avoiding the use of any photoresist to obtain the desired patterns. [25]

In 1996, Warren W. Flack et al. [26] studied the development rate characteristics and lithographic performance for two commercial photosensitive polyimide products. The two polyimide materials had very different process characteristics; one of the polyimide materials is based on the chemistry developed by Siemens while the other material is based on the Toray chemistry. SEM profile analysis, Bossung plots, and film retention plots were used to establish relative lithographic capabilities. Bossung plots of both types of polyimide showed that the type A material has a larger focus and exposure latitude than the type B material. The type A material demonstrated 12  $\mu\text{m}$  depth of focus with a 20 percent exposure latitude for 6  $\mu\text{m}$  lines with  $\pm 10$  percent CD control limits. In comparison, the type B polyimide exhibited 10  $\mu\text{m}$  depth of focus and 10 percent exposure latitude. However, the process latitude of the type B material has the potential to be improved if the manufacturer recommended high speed dispense nozzle was implemented. SEM analysis indicated that the type A material had substantially better sidewall angles and line edge roughness. The sidewall profiles indicated different problems for both type of materials at large positive defocus values. This suggested that

the focus should be set slightly negative for both types of materials to maintain vertical wall profiles.

In 2004, Steve Lien-Chung Hsu et al. [27] reported the preparation and properties of novel negative-working aqueous base developable PSPI compositions that consisted of polyimide precursors bearing phenolic hydroxyl groups and acrylate groups, a photoinitiator, a photosensitizer, a crosslinker and a solvent. Poly(amic esters) (PAEs) could be used as the precursors of negative-working, which prepared by direct polymerization of using phenylphosphonic dichloride (PPD) as an activator. Their structures were characterized by Fourier transform infrared spectroscopy (FTIR) and  $^1\text{H}$  NMR. The photosensitive polyimide precursor containing PMDA-75% BisAPAF-25% ODA-HEMA copoly(amic ester), MK/TBPS and tetra(ethylene glycol) diacrylate showed a sensitivity ( $D_g^{0.5}$ ) of  $452 \text{ mJ/cm}^2$ , and a contrast of 1.11 in a 3 mm film. A pattern with a resolution of 10 mm was obtained from this composition.

In 2007, Le Thu T. Nguyen et al. [24] synthesized poly(amic ester) (PAE) from pyromellitic dianhydride (PMDA), 2-hydroxyethylmethacrylate (HEMA) and 4,4'-oxydianiline (ODA) via the direct polymerization method using phenyl phosphonic dichloride (PPD) as an activator. Main parameters of the synthesis procedure were investigated by differential scanning calorimetry (DSC) analyses. Characteristics of the synthesized PAE and the imidized film were studied by the means of DSC, thermalgravimetric analyses (TGA) and Fourier transform infrared spectroscopy (FTIR). TGA measurements showed the imidized film obtained a high thermal stability. The 5 wt% loss occurred at a relatively high temperature of over  $500^\circ\text{C}$ . Thermal degradation mainly took place above  $600^\circ\text{C}$ . There was still 50 wt% left at  $700^\circ\text{C}$ . Additionally, formulations of photo-PAE and the Irgacure 369 as photoinitiator were prepared and photocuring was tested by lithography. The results showed that the photoinitiator Irgacure 369 was sufficient enough for the photocuring of PAE system. As a consequence images could be transferred to the PAE films by selective exposing to give patterns from the negative resist photo-PAE.

In 2010, Seunghyuk Choi et al. [28] studied the photoinitiator-free photosensitive polyimides with lower dielectric constant, prepared by reaction of fluorine aromatic diamine, 2,2'-bis(3-amino-4-hydroxyphenyl)hexafluoropropane

diamine (AHHFP) with 3,3',4,4'-benzophenonetetracarboxylic dianhydride (BTDA) and a mixture of various mole ratios of BTDA and 4,4'-(hexafluoroisopropylidene)diphthalic anhydride (6FDA) by using solution polycondensation reaction at room temperature and further imidization at 180 °C. The aromatic polyimides were further acrylated via a reaction with acryloyl chlorides in the presence of triethyl amine to produce negative photoinitiator-free PSPIs. All of the samples were characterized for the structure of polyimide by FTIR and NMR. While their morphologies were evaluated by XRD. These polyimides exhibited excellent solubility in all the organic solvents of this study at room temperature. The glass transition temperatures ( $T_g$ ) of all PSPIs were more than 250 °C as measured by DSC, and they exhibited good thermo-oxidative stability. The polymer films also showed high optical transparency and low dielectric constants. These newly synthesized PSPIs were evaluated to determine their electrical, thermal, and photolithographic properties. The PSPI (AHHFP-BTDA-6FDA [1 : 0.5 : 0.5] with high mole ratio of 6FDA showed lower dielectric constants of 2.420 at 1 kHz and 2.170 at 1 MHz in capacitance and optical methods, respectively. Further, the acrylated AHHFP-BTDA showed the highest photosensitivity than other PSPIs.

Due to their applications of photosensitive polyimides on optoelectronic devices were importantly limited because large volume shrinkage after curing from eliminating pendant photosensitive moieties. Such large volume shrinkage would cause a significant distortion on the patterned feature. [6] Hence, the reduction of volume shrinkage for photosensitive polyimide had become the major product. There were many people studied about photosensitive polyimides with silica hybrid, which some details were explained as follows

In 2005, Yu-Wen Wang et al. [29] studied the volume shrinkage of photosensitive poly(4,4'-(hexafluoroisopropylidene)diphthalic anhydride)-co-oxydianiline) (6FDA-ODA)/MDAE was largely reduced by photocrosslinking MDAE with a coupling agent and the silica domain in the hybrid materials. The used coupling agents were 3-methacryloxypropyl trimethoxysilane (MPTMS) or (4-vinylphenethyl)trimethoxysilane (VPTMS). The coupling agent and the silica domain were designed primarily for reducing the volume shrinkage and enhancing the thermal

properties, respectively. The retention of MDAE in the prepared hybrid films was supported by X-ray photoelectron spectroscopy (XPS) and thickness variation during curing process. The silica domain in the hybrid materials from TEM analysis was in the range of 10–50 nm, which was formed by the coupling agent and tetramethoxysilane. The silica domain significantly enhanced the thermal properties of the prepared hybrid films in comparison with parent fluorinated polyimide, including the glass transition temperature and coefficient of thermal expansion. The prepared hybrid materials also exhibited reduced refractive index and optical loss by increasing the silica. The SEM diagram suggested the prepared photosensitive hybrid materials could obtain lithographical patterns with a good resolution. These results indicated that the newly prepared photosensitive polyimide/silica hybrid materials might have potential applications for optical devices.

In 2009, Yang-Yen Yu et al. [30] studied the photopatternable fluorinated polyimide/silica hybrid materials were synthesized by 4,4'-hexafluoroisopropylidene diphthalic anhydride (6FDA), oxydianiline (ODA), aminopropyltriethoxysilane (APrTEOS), and 12 nm colloidal silica with a coupling agent. The monodispersed colloidal silica was used to form a silica domain instead of alkoxysilanes in the conventional process. The coupling agents used were 3-methacryloxypropyl trimethoxysilane (MPTMS) or (4-vinylphenethyl)trimethoxysilane (VPTMS). The coupling agent and the silica domain were designed to reduce the volume shrinkage and enhance the thermal properties, respectively. The retention of 2-methyl acrylic acid 2-dimethylamino-ethyl ester (MDAE) in the prepared hybrid films was supported by X-ray photoelectron spectroscopy (XPS) and thickness variation during the curing process. The particle size of silica in the hybrid materials based on SEM analysis was in the range of 10-25 nm. The prepared hybrid materials also exhibited a reduced refractive index after increasing the silica content. The SEM diagram suggested the prepared photosensitive hybrid materials could obtain lithographical patterns with a good resolution. These results indicated that the newly prepared photosensitive polyimide/silica hybrid materials might have potential applications for optical devices.

In 2010, Suttisak Srisuwan et al. [13] synthesized Photosensitive polyimide/silica hybrid materials by reaction between 4,4'-hexafluoroisopropylidene

diphthalic anhydride (6FDA) and 4,4'-oxydianiline. The inter-chain chemical bonding and the inter-chain hydrogen bonding between the polyimide and silica moieties were increased by the incorporation of 2-(dimethylamino) ethyl acrylate and 3-aminopropyl trimethoxysilane, respectively. The photoinitiator was bis(2,4,6-trimethyl benzoyl) phenylphosphine oxide (Irgacure-819). The various coupling agents were utilized included tetrakis (allyloxy) silane (TAL). Most silica hybrid films showed better volume shrinkage and temperature resistance. The cooperation of octavinyl POSS, as the coupling agent, could lower dielectric constant ( $k$ ) down to 2.48 but with the poorer volume shrinkage and temperature resistance than the other silica hybrid films. The addition of tetramethyl orthosilicate and 3-methacryloxy propyltrimethoxysilane with silica content of 5.6 wt % can reduce dielectric constant down to 2.26 but with worse volume shrinkage than the incorporation with TAL. The TAL hybrid film with degree of polymerization of 25 showed the best properties that optimized photolithography, dielectric constant ( $k = 3.81$ ), volume shrinkage, and temperature resistance ( $T_{d5\%} = 378$  °C.) with only 0.22 wt % silica content.

In 2011, Yu-Wen Wang et al. [31] synthesized the new non-fluorinated colorless photosensitive polyimide-silica hybrid optical materials with relatively low large volume shrinkage, which could solve the poor dimensional stability in conventional ionic type photosensitive polyimide. The experimental results showed that the nano-silica domain and the crosslinked structures significantly enhanced the thermal properties, such as the glass transition temperature and coefficient of thermal expansion. The prepared hybrid film not only exhibited high transparency in the visible region but also had tunable refractive index, low birefringence and optical loss by introducing the silica moiety. The SEM image suggested the prepared photosensitive hybrid materials could obtain fine lithographical patterns with an excellent dimensional stability. The combination of excellent optical properties and dimensional stability suggested the potential applications of the prepared hybrid materials for optoelectronic device applications.

## **CHAPTER IV**

### **EXPERIMENTS**

This chapter describes details of experiment performed in this research. There comprised five main parts, which described all utilized material and chemicals as shown in section 4.1. Details of the synthesis of negative photosensitive polyimide, equipment and characterization of polyimide film are explained in section 4.2, 4.3 and 4.4. The benefits of this research and schedule were interpreted in section 4.5 and 4.6, respectively.

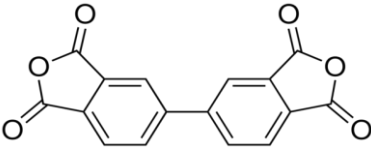
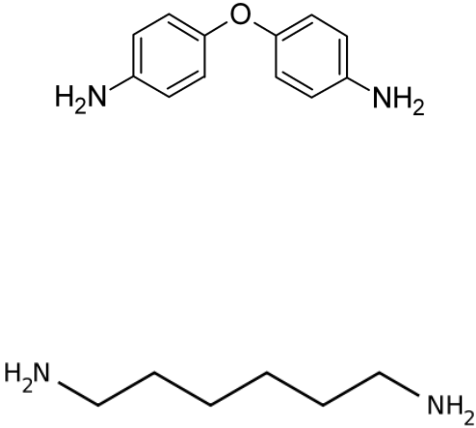
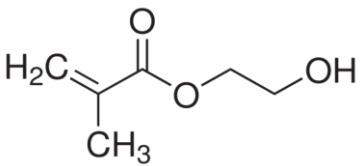
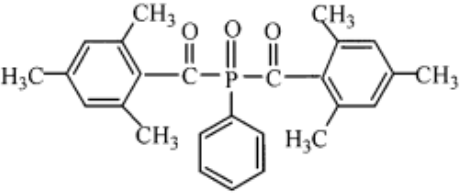
#### **4.1 Materials and chemicals**

1. 3,3',4,4'-biphenyltetracarboxylic dianhydride (BPDA) purchased from Aldrich chemical Company, Inc.
2. 4,4'-oxydianiline (ODA) purchased from Aldrich chemical Company, Inc.
3. Hexamethylenediamine (HMDA) purchased from Aldrich chemical Company, Inc.
4. 4-aminobenzenethiol purchased from TCI America.
5. Octavinyl POSS purchased from Hybridplastics Company, Inc.
6. 2-hydroxyethyl methacrylate (HEMA) purchased from Merck Ltd., Thailand.
7. Bis (2,4,6-trimethylbenzoyl) phenyl phosphine oxide (Irgacure-819) was grateful provided by Ciba Specialty Chemical Thailand.
8.  $\gamma$  – butyrolactone purchased from Aldrich chemical Company, Inc.
9. *N*-methyl-2-pyrrolidinone (NMP) purchased from Merck Ltd., Thailand.
10. Copper clad was gratefully provided by Mektec Manufacturing Corporation (Thailand) Ltd.

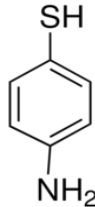
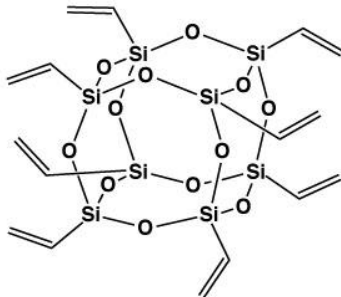
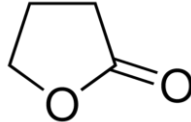
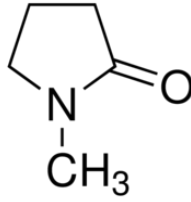
All of them were used without purification.

The chemical structures can be demonstrated in Table 4.1

**Table 4.1** Chemical structures of materials used in this research

Materials	Chemical structures
<p><b>Dianhydride</b></p> <ul style="list-style-type: none"> <li>- 3,3',4,4'-biphenyltetracarboxylic dianhydride (BPDA)</li> </ul>	
<p><b>Diamine</b></p> <ul style="list-style-type: none"> <li>- 4,4'-oxydianiline (ODA)</li> <li>- Hexamethylenediamine (HMDA)</li> </ul>	
<p><b>Photosensitive precursor</b></p> <ul style="list-style-type: none"> <li>- 2-hydroxyethyl methacrylate (HEMA)</li> </ul>	
<p><b>Photosensitive initiator</b></p> <ul style="list-style-type: none"> <li>- Bis (2,4,6-trimethylbenzoyl) phenyl phosphine oxide (Irgacure-819)</li> </ul>	

**Table 4.1** Chemical structures of materials used in this research (con't)

Materials	Chemical structures
<p data-bbox="284 472 507 510"><b>Click chemistry</b></p> <ul data-bbox="331 577 657 1055" style="list-style-type: none"><li data-bbox="331 577 657 616">- 4-aminobenzenethiol</li>          <li data-bbox="331 1016 596 1055">- Octavinyl POSS</li></ul>	<div data-bbox="1114 528 1209 734" style="text-align: center;"> <chem>Nc1ccc(S)cc1</chem></div> <div data-bbox="995 882 1337 1178" style="text-align: center;"> <chem>C=CC12[Si](O1)O[Si](O2)C=C</chem></div>
<p data-bbox="284 1270 405 1308"><b>Solvents</b></p> <ul data-bbox="331 1375 820 1854" style="list-style-type: none"><li data-bbox="331 1375 608 1413">- <math>\gamma</math> - butyrolactone</li>          <li data-bbox="331 1816 820 1854">- <i>N</i>-methyl-2-pyrrolidinone (NMP)</li></ul>	<div data-bbox="1066 1330 1257 1451" style="text-align: center;"> <chem>O=C1OCCC1</chem></div> <div data-bbox="1066 1711 1257 1912" style="text-align: center;"> <chem>CN1C(=O)CCC1</chem></div>



## **4.2 Synthesis of the negative photosensitive polyimide**

### **4.2.1 Preparation of the negative photosensitive poly (amic acid)**

Poly (amic acid) was synthesized by the 3,3',4,4'-biphenyltetracarboxylic dianhydride (BPDA) with hexamethylenediamine (HMDA) and 4,4'-oxydianiline (ODA) at stoichiometric dianhydride/diamine ratio of 100:30:70 in *N*-methyl-2-pyrrolidinone (NMP) solutions. The thickness was controlled by the usage of calculated amount of solution of poly (amic acid). The mixture solutions were each stirred by magnetic stirrer for 30 min under argon atmosphere to obtain the poly (amic acid). After that, 2-hydroxyethyl methacrylate (HEMA) photosensitive precursor and Bis (2,4,6-trimethylbenzoyl) phenyl phosphine oxide (Irgacure-819) photosensitive initiator were added into the mixture solutions. Poly (amic acid) was then became negative photosensitive poly (amic acid). Preparations of the negative photosensitive poly (amic acid) can be showed in Figure 4.1.

### **4.2.2 Preparation of the negative photosensitive poly (amic acid) incorporate with click chemistry**

Poly (amic acid) was prepared by the same method as the topic 4.2.1 but also used click chemistry to prepare the end group of molecules with 4-aminobenzenethiol and double bond binding the double bond of end group of octavinyl POSS. Then 4-aminobenzenethiol at calculated ratio was added in polyamic acid solution follows by Octavinyl POSS at stoichiometric ratio before the addition of HEMA and Irgacure-819. Preparations of the negative photosensitive poly (amic acid)/silica hybrids can be showed in Figure 4.2

### **4.2.3 Patterning of the negative photosensitive polyimide**

The negative photosensitive poly (amic acid) precursors from both methods were cast onto copper substrate. The film was dried at 55 °C for 2 hour then exposed to the UV light through a transparent mask (size of mask 5x5, 4x4 3x3 and 2x2 mm) for 200 second and developed by  $\gamma$  – butyrolactone (50 ml) for 2 min. Finally, the developed pattern was cured by the multi-step heating process of 100, 150, 200 and 250 °C for 30 min in the vacuum oven. The negative photosensitive polyimide film was obtained as product.

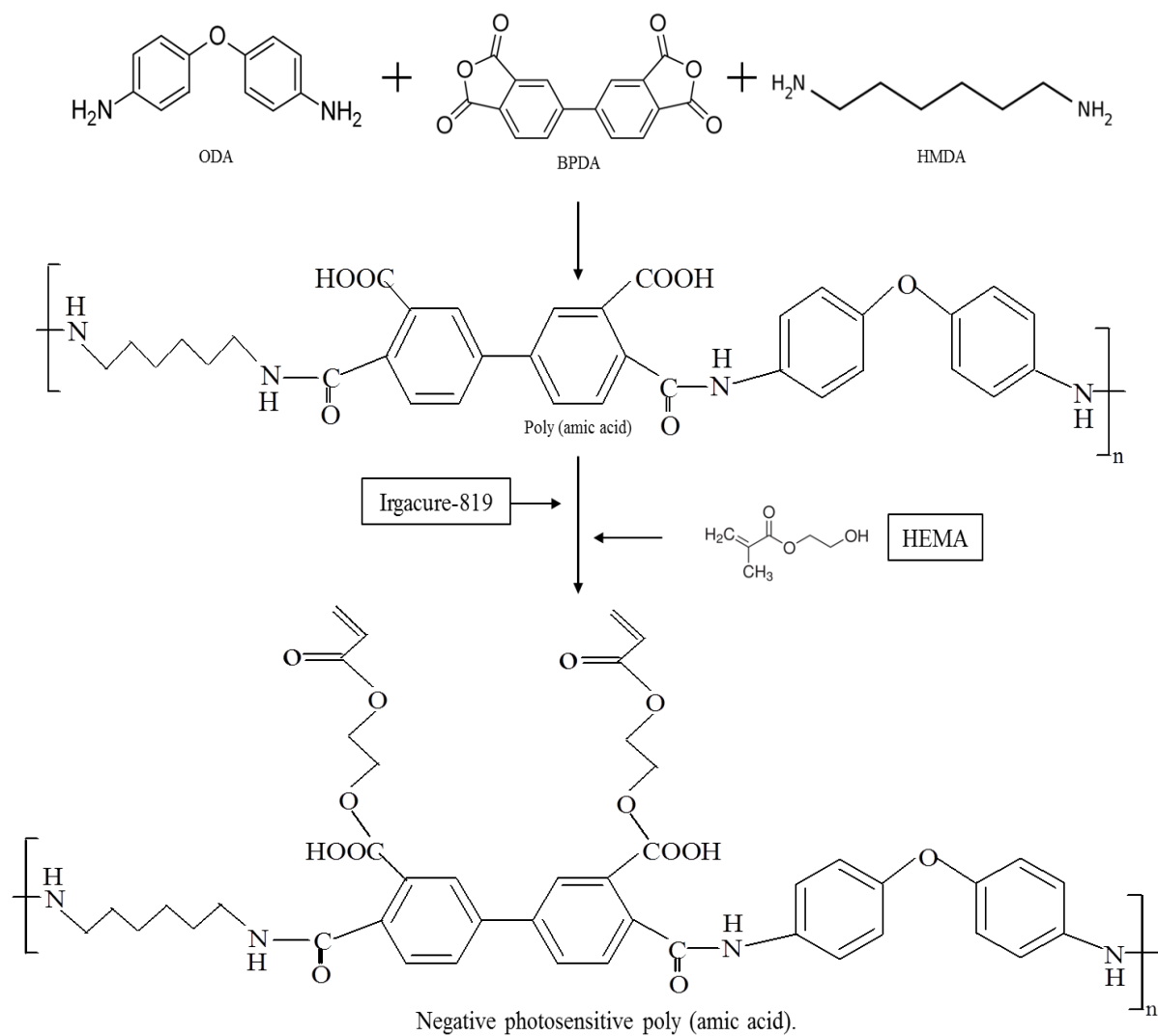


**Figure 4.1** Preparation of negative photosensitive poly (amic acid)

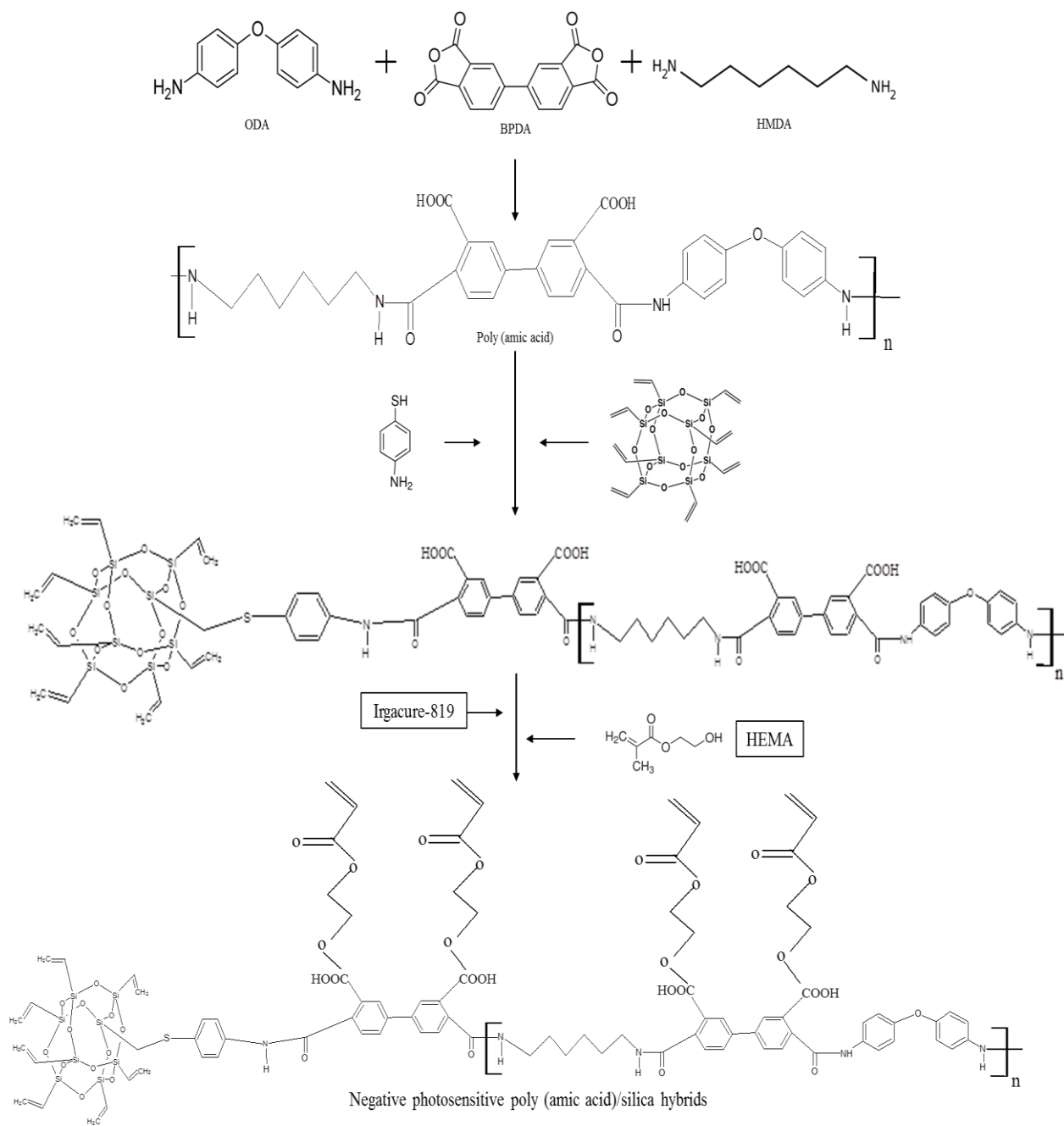


**Figure 4.2** Preparation of negative photosensitive poly(amic acid)/silica hybrids

## 4.3 Equipment

### 4.3.1 Glove box

Glove box was used with oxygen and moisture analyzer for keeping air-sensitive reagents and handling solid reagents under argon atmosphere. Typically the oxygen and moisture levels in the glove box are controlled at about 0.1 ppm. The glove box is shown in Figure 4.3



**Figure 4.3** Glove box

### 4.3.2 Vacuum oven

Vacuum oven was used for evaporation of solvent from films and used for curing of the negative photosensitive polyimide. The pressure inside the oven was controlled under vacuum. The vacuum oven can be shown in Figure 4.4.

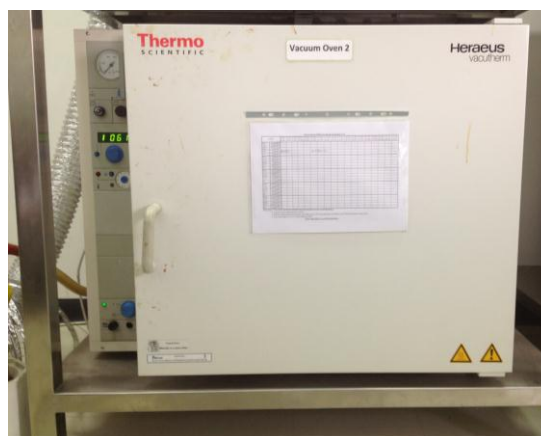


**Figure 4.4** Vacuum oven

### 4.3.3 UV lamp

UV lamp was used for photochemical process by UV radiation. In this research, UV light from UV lamp was used for photo crosslinking of polyimide with photo precursor. When measured with a UV meter, the intensity of light is  $1.76 \text{ mW/cm}^2$ . The UV lamp and UV meter are shown in Figure 4.5 and 4.6, respectively.



**Figure 4.5** UV lamp



**Figure 4.6** UV meter

### 4.3.4 Magnetic stirrer and hot plate

Magnetic stirrer and hot plate were used for mixing solvent with chemicals. The hot plate model was RCT basic from IKA Labortechnik.

#### **4.3.5 Laboratory bottles, Syringe, Needle and Glass Substrate**

Sizes of the laboratory bottles were 25, 50 and 100 ml. The syringes used in these experiments had a volume of 0.5, 1 and 10 ml. The glass mirrors substrates were used for cast films in order to check properties of polyimide films.

#### **4.3.6 Transparent mask**

Transparent mask was used for unexposed UV area. Sizes of the transparent mask used in these researches were 5x5, 4x4, 3x3 and 2x2 mm. The transparent mask was shown in Figure 4.7

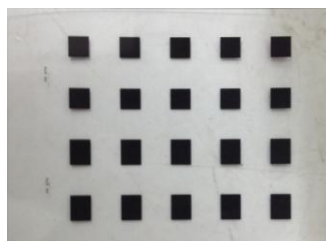


**Figure 4.7** Transparent mask

## 4.4 Characterization Instruments

### 4.4.1 Fourier transform infrared spectroscopy (FTIR)

FTIR spectrometer was used for characterization of the functional groups of polyimide such as amine group and anhydride group. So, the structures of polyimide were confirmed by FTIR. Infrared spectra were recorded with Nicolet 6700 FTIR spectrometer and range of scanning from 400 to 4,000  $\text{cm}^{-1}$  with scanning times of 64.



**Figure 4.8** Fourier transform infrared spectroscopy (FTIR) Equipment

### 4.4.2 Nuclear magnetic resonance spectroscopy ( $^1\text{H}$ -NMR)

NMR spectrometer was used for characterization of the different types of hydrogen atoms in 4-aminobenzenethiol and Octavinyl POSS, which were click chemistry. Spectra were recorded with Bruker 400 Ultra Shield<sup>TM</sup> NMR spectrometer and range of scanning from 0 to 14 ppm with number of scan of 1,024. The solvent used in these experiments was dimethyl sulfoxide (DMSO).



**Figure 4.9** Nuclear magnetic resonance spectroscopy (NMR) Equipment

#### 4.4.3 Thermogravimetric analysis (TGA)

The thermal stability or thermal decomposition of the polyimide films was analyzed by TGA. Thermograms were performed using a Diamond TG/DTA Thermogravimetric/Differential Thermal Analyzer. The sample weights were 2-5 mg. The sample weights would change according to temperature ramp. The temperature range of 50-800°C at a heating rate of 10°C/min with nitrogen purge flow rate 100 ml/min was used.

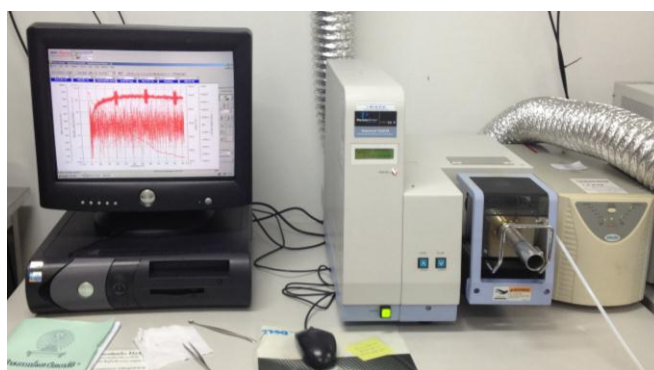


**Figure 4.10** Thermogravimetric analysis (TGA) Equipment

#### 4.4.4 LCR meter

The LCR meter was used to determine the dielectric properties of the polyimide films. The dielectric properties were measured at room temperature, 1 kHz and 1V with Agilent E4980A Precision LCR meter. The dielectric constants were obtained via the capacitance method.



**Figure 4.11** LCR meter Equipment



#### 4.4.5 Tensile testing machine

The tensile properties of the polyimide films were characterized using a universal testing machine with model of dual column tabletops. Sample size 2x5 cm and a test speed of 5 mm/min were used. The tests were preceded according to ASTM D 882-02.



**Figure 4.12** Tensile testing machine Equipment

#### 4.4.6 Confocal microscope

Confocal microscope could be analyzed surface characteristic and lithographic formed on surface of polyimide. The polyimide films were characterized using a confocal laser scanning microscope with model of Olympus OLS3000. In this research, the morphology of the polyimide films was measured by Confocal Microscope with magnification of 5x.



**Figure 4.13** Confocal microscope Equipment

#### 4.4.7 Optical microscope

Optical microscope could be observed and photograph specimen. The polyimide films were characterized using an optical microscope with model of SZX-1LLD2-200. In this research, the lithographic formed on surface of polyimide were roughly analyzed.



**Figure 4.14** Optical microscope Equipment

#### 4.4.8 Stylus profiler

Stylus profiler was used to determine the thickness and the size opening of the polyimide films. The polyimide films were characterized using a stylus profiler with model of Dektak 150 and brand of Veeco.



**Figure 4.15** Stylus profiler Equipment

#### 4.4.9 Micrometer

Micrometer was used for measurement of the thickness of the polyimide films. The polyimide films were characterized using an electronic digital micrometer stylus with the measuring range, resolution and accuracy of 0-25 mm, 0.001 mm and 0.002 mm, respectively.



**Figure 4.16** Micrometer Equipment

#### 4.5 Benefits of this research

4.5.1 Obtain synthesis process for ultra-thick negative photosensitive polyimide.

4.5.2 Obtain another method for lower shrinkage negative photosensitive polyimide preparation.

4.5.3 Obtain ratio of mask to opening of ultra-thick negative photosensitive polyimide films and photo-mask size.

#### 4.6 Research methodology

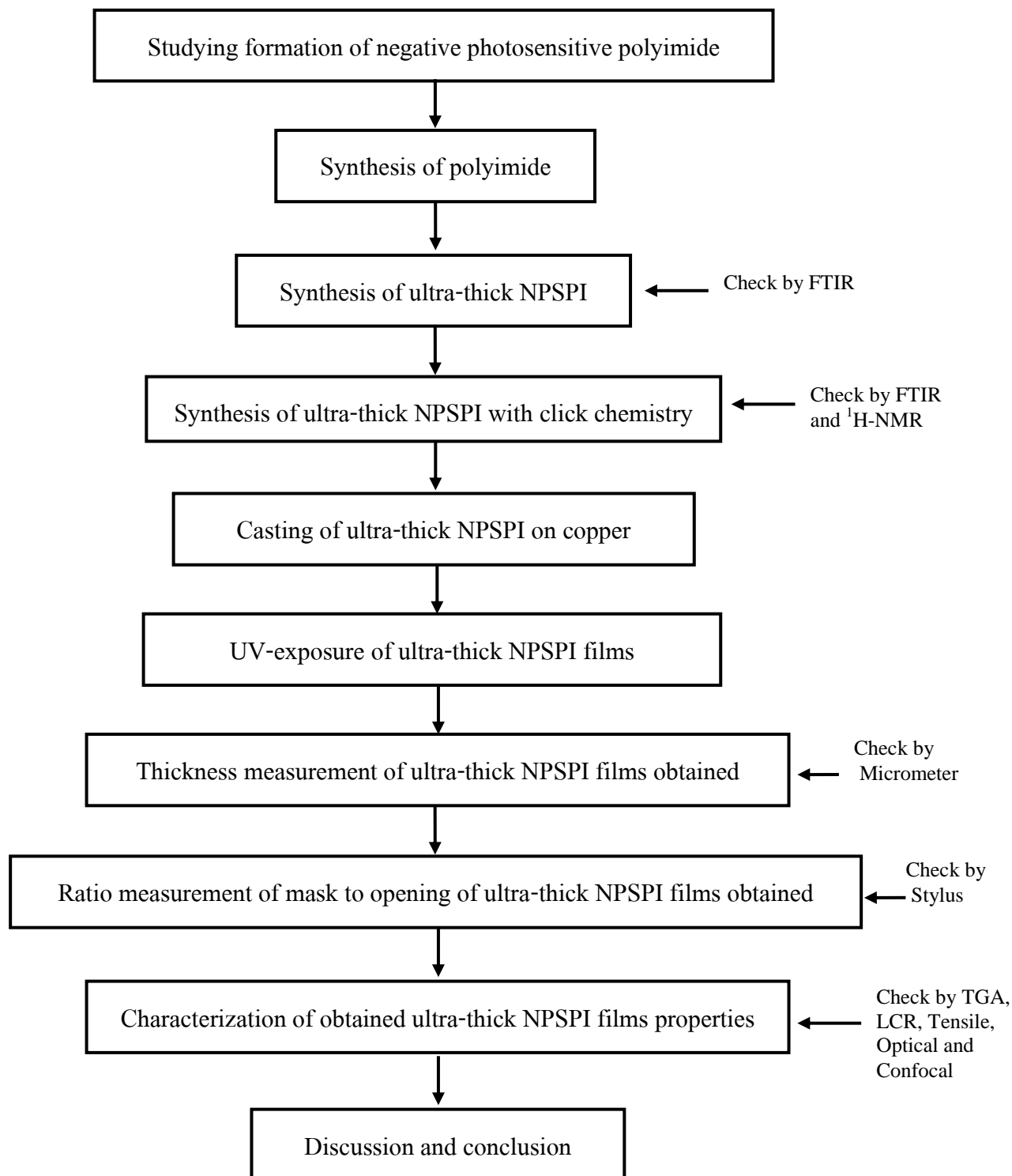


**Figure 4.17** Flow diagram of research methodology

## **CHAPTER V**

### **RESULTS AND DISCUSSION**

This chapter describes the details about the properties of the negative photosensitive polyimide and negative photosensitive polyimide/silica (POSS) hybrid materials synthesis. The films thickness and the relation between opening sizes of negative photosensitive polyimide films with photo-mask size were determined. In addition, the effects of the properties of the synthesized films such as thermal properties and dielectric properties were also investigated.

#### **5.1 Negative photosensitive polyimide (NPSPI) and negative photosensitive polyimide/silica (POSS) hybrid materials synthesis**

##### **5.1.1 Preparation of the negative photosensitive polyimide and negative photosensitive polyimide/silica (POSS) hybrid materials synthesis**

In this research, the negative photosensitive polyimide (NPSPI) were synthesized by 3,3',4,4'-biphenyltetracarboxylic dianhydride (BPDA) with hexamethylenediamine (HMDA) and 4,4'-oxydianiline (ODA) at stoichiometric dianhydride/diamine ratio of 100:30:70 in *N*-methyl-2-pyrrolidinone (NMP) solutions to form poly(amic acid) while the negative photosensitive polyimide/silica (POSS) hybrid materials were prepared by the same method in form of the poly (amic acid) but also use click chemistry with 4-aminobenzenethiol and the double bond binding end groups of Octavinyl POSS. Then 4-aminobenzenethiol at calculated ratio was added in polyamic acid solution, followed by Octavinyl POSS at stoichiometric ratio of 1:1. After that, 2-hydroxyethyl methacrylate (HEMA) photosensitive precursor and Bis (2,4,6-trimethylbenzoyl) phenyl phosphine oxide (Irgacure-819) photosensitive initiator were added into the mixture solutions.

### 5.1.2 Function of the components

The main materials are the BPDA, HMDA and ODA that cooperated as the oligomer polyimide base materials. The degrees of polymerization (DP) are 63, 63 and 200 monomers per molecule of polyimide. The small size of the polyimide oligomer has the advantage in the adhesion to the substrates and in the easier solubility in the developing solvents. However, the larger molecules are precious for the higher tensile strength and the less volume shrinkage of the photosensitive polyimide which is essential for the utilization of the films.

The mechanism of the negative photosensitive started by the reaction of the HEMA with the ionic bonds that linked the oxygen of HEMA with the free carboxylic from the BPDA molecules. The main photosensitive polyimide started from the polyamic acid of BPDA, HMDA and ODA that two carboxylic bonds will react with HMDA and ODA as the skeleton, and the two others carboxylic bonds will react with HEMA to be the photosensitive junctions. The expose to UV light cause the dissociation of the Irgracure molecules into free radicals when started the free radical polymerization of the double bonds in the system. The unsaturated bond of HEMA will be attacked and open the linkages with each other that result in the cross-linked over the polyamic acid skeleton molecules (Figure 5.1). The expose system to UV light will be harder to dissolve by developing solvents while the unexposed area will be polyamic acid without the cross-linked that will enable to dissolve in the developing solvent. The unexposed part will be wash away with the developing solvent, while the exposed area will remain hardly dissolve with the developing solvent. Thus, this phenomenon showed the Negative resist photosensitive materials.

The final curing of the cross-linked polyamic acids, which remain after the dissolve by developing solvents, will finally break the ionic bond of the cross-linked double bond of HEMA from ring closer of polyimides. This excluded cross-linked polymer will be evaporated away from polyamic acid at high temperature during the imidization, so it will cause the high volume shrinkage of the photosensitive polyimide after final cure. Many successful attempt of silica hybrid can reduce the shrinkage of photosensitive polyimide up to around 6-8 percent [13,29-30] However, the usage of octavinyl POSS (Polyhedral silsesquioxane) as the effective silica hybrid for this purpose has been investigated by S.Srisuwan et. all [13] before,

but the usage was detrimental to the properties of NPSPI. Thus, to find the benefits from octavinyl POSS for NPSPI was the main theme of the research. The 4-aminobenzenethiol is the hybrid material consisted of amine end-chain, aromatic structure and the end-chain silicon with hydrogen. 4-aminobenzenethiol would take part together with octavinyl POSS in the reaction of the double bonds of the octavinyl POSS with the matrix of HEMA double bonds in order to reduce the shrinkage of the photosensitive polyimide during the last curing after developing by solvents (Figure 5.2) and found the possibility of reducing dielectric constant of PSPI.

Octavinyl POSS consists eight double bonds as ligands. The hybrid molecules expected to supply better mechanical, thermal and dielectric properties to the polyimide. In this research, the effect of octavinyl POSS to the properties of the negative photosensitive polyimide would be investigated as in the following section.

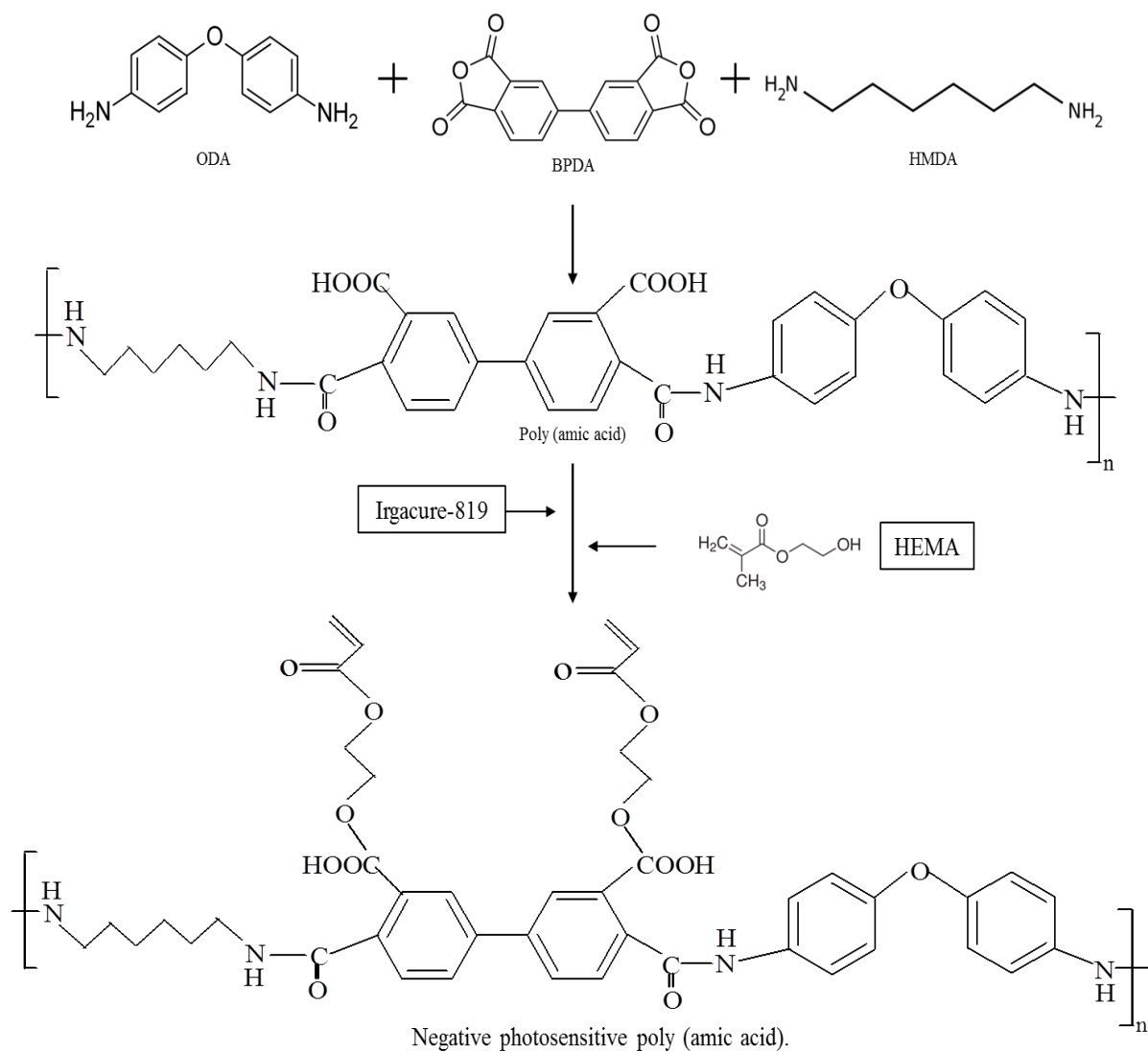


**Figure 5.1** Preparing negative photosensitive poly (amic acid)



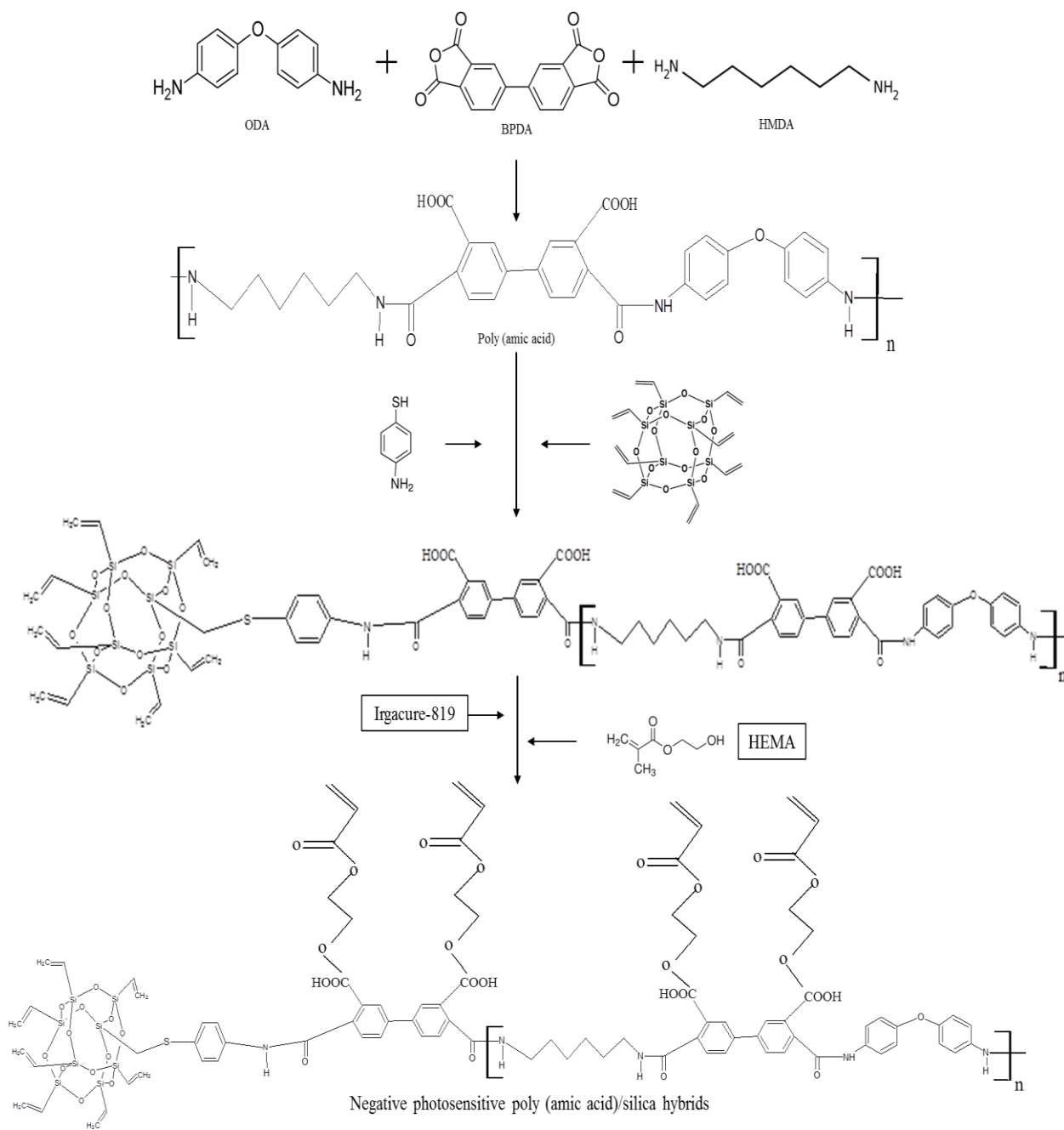


**Figure 5.2** Preparing negative photosensitive poly(amic acid)/silica hybrids

### 5.1.3 FTIR spectrum of PI, NPSPI and NPSPI/silica hybrids films

Figure 5.3 shows the FTIR spectrum of polyimide (PI) and negative photosensitive polyimide (NPSPI) film after curing. The imide characteristic absorption bands of the prepared materials were further evidenced by the following absorption bands;  $1778\text{ cm}^{-1}$  (C=O sym. str.);  $1726\text{ cm}^{-1}$  (C=O asym. str.); and  $1380\text{ cm}^{-1}$  (C–N str.). The Si–O–Si stretching bands around  $1100\text{ cm}^{-1}$  [32] of NPSPI/silica hybrids was stronger than that of PI or NPSPI implied the higher silica content. The C–NH ( $1660\text{ cm}^{-1}$ ) characteristic absorption bands of the poly(amic) acid disappeared from the spectra, indicating that the imidization reactions were completed. In this research the peak at  $1500\text{ cm}^{-1}$  state the benzene rings C=C was used as base peak for determination of the amount of silica in the systems by the ratio of the peak at  $1100\text{ cm}^{-1}$  to the  $1500\text{ cm}^{-1}$ . Table 5.1 shows the wave number ratios of (1100/1500). From results, it was found that NPSPI have the ratio higher than the nascent PI, which, from theory, NPSPI should have the same ratio with PI because both NPSPI and PI had no silica in the systems. From the inspection of NPSPI system, the peak at about  $1100\text{ cm}^{-1}$  also represented the peak of C–O in HEMA molecules (photo precursor) which some of HEMA molecules may be not evaporated away from poly(amic) acid after curing.[33] In NPSPI/silica hybrids that comprised POSS, the ratio was higher than PI and NPSPI because incorporation of octavinyl POSS in polyimide molecules. Moreover, the peak at  $1500\text{ cm}^{-1}$  stated the benzene rings C=C in NPSPI/silica hybrids that included the benzene rings C=C of 4-aminobenzenethiol. Nevertheless the silica content of NPSPI/silica hybrids system was still higher than PI and NPSPI system even the divider, was increased.

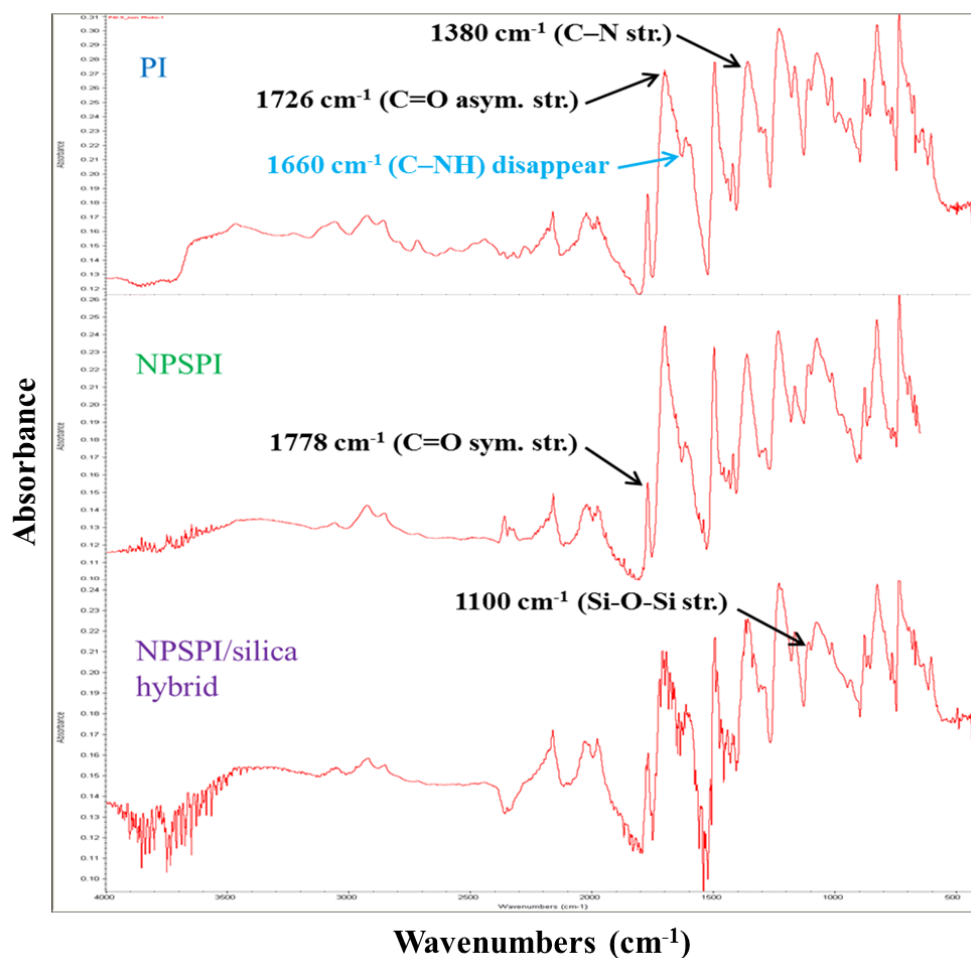


**Figure 5.3** FTIR spectra of prepared films, PI, NPSPI and NPSPI/silica hybrids

**Table 5.1** The wave number ratio of (1100/1500) of PI, NPSPI and NPSPI/silica hybrids

Type of polyimide films	Wave number ratio of (Si/C=C)	POSS (mol)
PI	0.772	0.000
NPSPI	0.815	0.000
NPSPI/Silica hybrids	0.972	0.020

### 5.1.4 $^1\text{H-NMR}$ of 4-aminobenzenethiol, Octavinyl POSS and 4-aminobenzenethiol incorporated with Octavinyl POSS

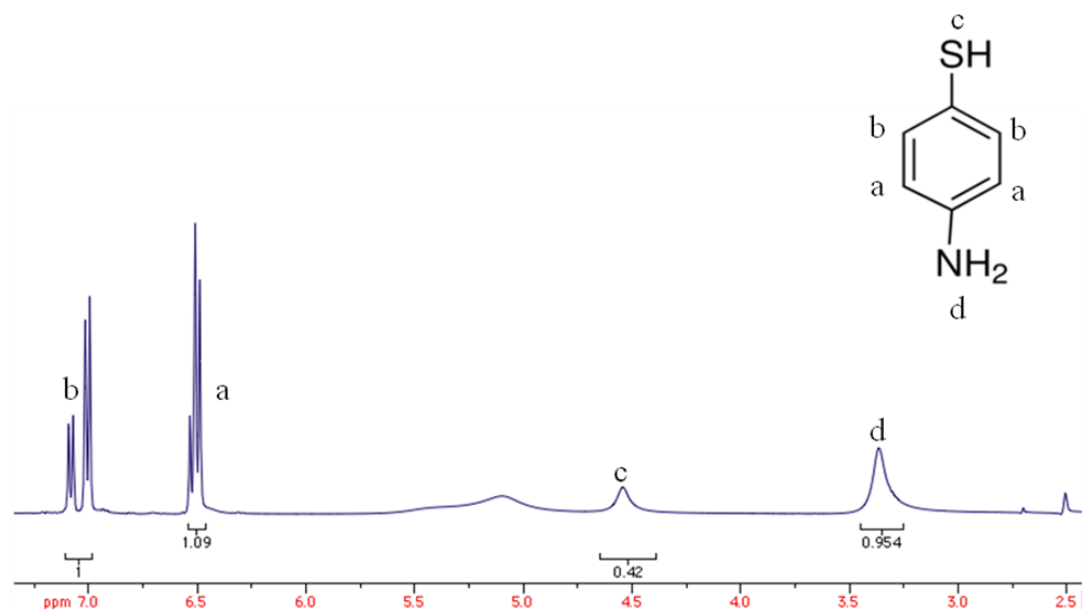


Figure 5.4  $^1\text{H-NMR}$  of 4-aminobenzenethiol

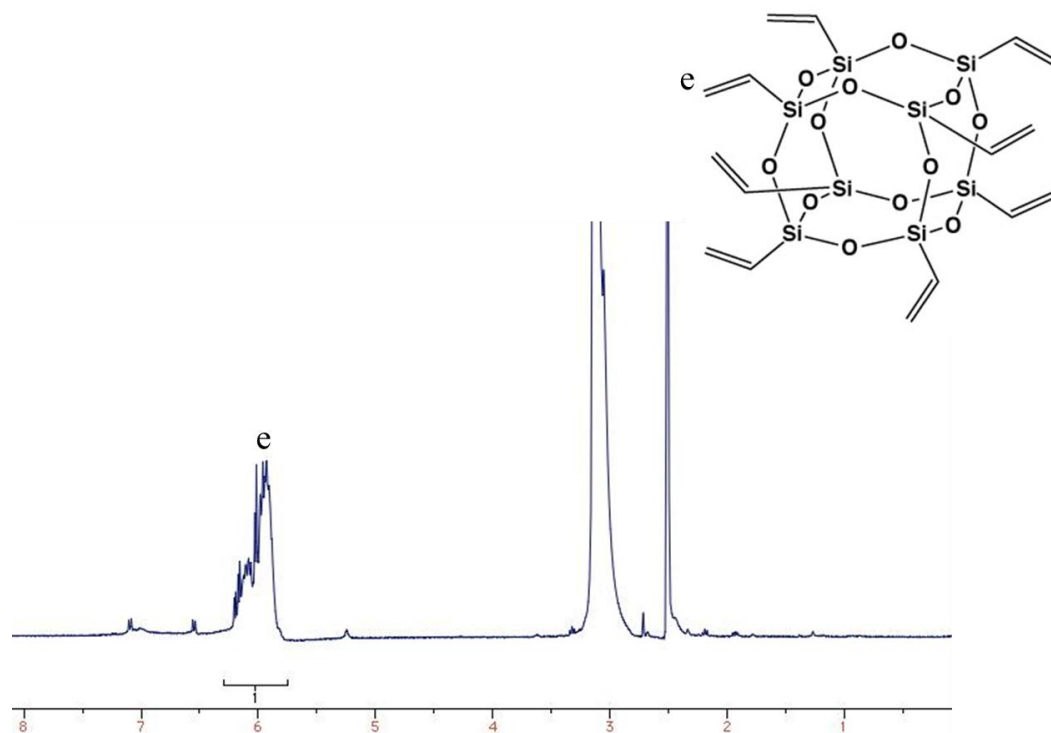
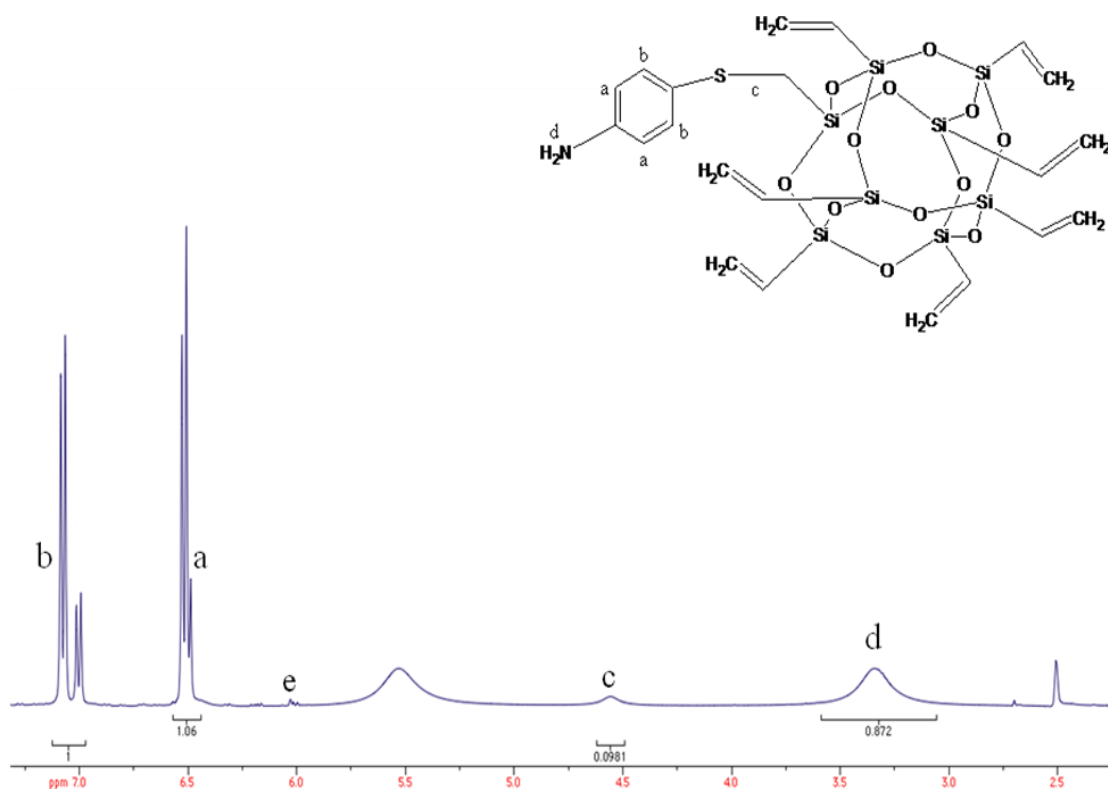


Figure 5.5  $^1\text{H-NMR}$  of Octavinyl POSS



**Figure 5.6**  $^1\text{H-NMR}$  of 4-aminobenzenethiol incorporated with Octavinyl POSS

$^1\text{H-NMR}$  was used for characterization of the different types of hydrogen atoms in 4-aminobenzenethiol and Octavinyl POSS, which were the ingredients of click chemistry. The solvent used in these experiments was dimethyl sulfoxide (DMSO). The total results could be shown in Figure 5.4-5.6. From Figure 5.4, two sharp bands around 6.5 ( $\text{H}_a$ ) and 7.2 ( $\text{H}_b$ ) ppm corresponded to protons of the benzene ring of 4-aminobenzenethiol. The peak at around 3.3 ( $\text{H}_d$ ) and 4.5 ( $\text{H}_c$ ) ppm were assigned to the proton of  $\text{NH}_2$  and  $\text{SH}$  groups in 4-aminobenzenethiol, respectively. [33-34]. For the pure Octavinyl POSS, the resonance band of vinyl protons is observed at around 6.0 ppm as multiple peaks because of the coupling of hydrogen protons in Figure 5.5 [32,34-37]. Consequently, when 4-aminobenzenethiol was incorporated with Octavinyl POSS (Figure 5.6) then the proton of  $\text{SH}$  and vinyl protons of Octavinyl POSS disappeared, because of the reaction with double bond of Octavinyl POSS [38]. However, there are a few resonance bands at nearby 4.5 and 6 ppm, which belonged to the unreacted proton of  $\text{SH}$  and vinyl protons of Octavinyl POSS molecules, respectively.

## 5.2 Determination the thickness of the negative photosensitive polyimide films

**Table 5.2** Thickness of PI and NPSPI films

No.	Poly(amic acid) solution* (ml)	Film thickness after cured at 250 °C** (µm)	
		PI	NPSPI
1	0.4	24.1	12.3
2	0.5	27.7	22.0
3	1.0	42.4	39.7
4	1.5	67.4	56.6
5	2.0	85.9	72.3

\*Conc. of solution = 17.17% wt. /vol., Copper size = 5x5 cm

\*\* Measured by micrometer.

Table 5.2 shows the thickness of PI and NPSPI films after curing at 250 °C. When the amounts of droplets of poly(amic acid) solution cast on substrates (copper size = 5x5 cm) were increased, the thickness of the PI and NPSPI films were increased accordingly. However, the thicknesses of NPSPI films were thinner than PI films (at the same conditions) due to the loss of photo-cross-linking agents, 2-hydroxyethyl methacrylate (HEMA) and Igracure, after curing. At approximate, 0.4 ml of poly (amic acid) solution could make film's thickness about 12 micron, as required.

The experiment was repeated to confirm the thickness of the film that was about 12.5 microns by changing the size of the substrate (copper plate) from 5x5 cm to 10x10 cm and changing the poly(amic acid) solution from 0.4 ml to 1.6 ml. Experiment was repeated 3 times which the thickness of the NPSPI film obtained can be shown in Table 5.3. When the size of the substrate 5x5 cm was used, the thickness of the film after drying at 55 °C for 2 hr (prebake before exposed to UV) were in the range of 24 to 28 micron and after cured at 250 °C for 30 min the thickness of the film were in the range of 11-13 micron, the required thickness. After that the size of the substrate were changed to 10x10 cm the thickness of the film after drying at 55 °C for 2 hours were in the range of 24 to 26 micron and after curing at 250 °C for 30 min the

thickness of the film were in the range of 11-13 micron, the desired thickness. The standard deviation of the film on 5x5 cm plates was 0.34 and the standard deviation of the film on 10x10 cm plates was 0.49, which was narrow enough to have to good control by controlling polyamic acid solution.

**Table 5.3** Thickness of NPSPI films at various sizes of substrate.

No.	Size of copper plate	Poly(amic acid) solution* (ml)	Film thickness** (micron)	
			After dried at 55 °C	After cured at 250 °C
1	5x5 cm	0.4	26.50	11.83
2	5x5 cm	0.4	27.50	12.33
3	5x5 cm	0.4	24.17	11.67
4	10x10 cm	1.6	24.50	11.85
5	10x10 cm	1.6	25.17	12.50
6	10x10 cm	1.6	25.50	12.80

\* Concentration of PI = 17.17 % wt. /vol.

\*\* Measured by micrometer.

### 5.3 The effect of developing time on the dissolution in the developer of the negative photosensitive polyimide films

The negative photosensitive poly(amic acid) precursors were cast onto copper substrate. The films were dried at 55 °C for 2 hours, then exposed to the UV light through a transparent mask for 200 seconds and developed by  $\gamma$  – butyrolactone for 0, 30, 60, 90 120,150 and 180 seconds. To clarify the difference of dissolution behavior between the exposed and unexposed areas, the effect of developing time on the dissolution in the developer ( $\gamma$  – butyrolactone) was studied, and the results are shown in Table 5.4. The increasing of developing time made % dissolution of the unexposed areas to increase too. To confirm the thickness before exposed U.V. at various developing time then the average and the standard deviation of the thickness before exposed U.V. were determined which were 60.13  $\mu\text{m}$  and 1.27, respectively and the thickness before exposed U.V. at each developing time are in the range of 99.7% of

acceptable data. From the results, at developing time of 120 seconds was the best condition in this case because the unexposed areas were completely washed away with the developing solvent more than other conditions so % dissolution of polyimide films in the developing solvent was the highest. For at the developing time of 150 and 180 second, % dissolution of the exposed areas were higher than the other exposed areas because of the over developing time, because the exposed to UV area was also washed away more than acceptable limit. However, the thickness of unexposed areas after exposed U.V. at developing time of 120,150 and 180 second were 35.55, 35.77 and 35.65  $\mu\text{m}$  can be seen that % dissolution of the unexposed areas were high which acceptable. To confirm the thickness of the unexposed areas after exposed U.V. at developing time of 120,150 and 180 second which proved by the average and the standard deviation of the thickness of unexposed areas after exposed U.V. were 35.66  $\mu\text{m}$  and 0.11 (35.66 $\pm$ 0.33  $\mu\text{m}$ ), respectively and the thickness of unexposed areas after exposed U.V. at each developing time were in the range of 99.7% of acceptable data. The relation between % dissolution of the exposed and unexposed areas of polyimide films in the developing solvent with each developing time can be shown in Figure 5.7.

**Table 5.4** The thickness of NPSPI films and % dissolution at various developing time.

Developing time (s)	Film thickness* ( $\mu\text{m}$ )			Dissolution of NPSPI films (%)	
	Before exposed U.V.	After exposed U.V.		Exposed areas	Unexposed areas
		Exposed areas	Unexposed areas		
0	60.55	60.15	60.15	1.51	1.51
30	61.55	61.05	48.55	1.82	47.27
60	58.22	58.15	40.05	0.29	75.18
90	59.22	58.95	37.25	1.07	87.29
120	59.55	59.25	35.55	1.18	94.12
150	61.75	54.05	35.77	27.80	93.79
180	60.05	52.55	35.65	28.85	93.85

\* Include copper plate (thickness of copper = 34.05  $\mu\text{m}$ )



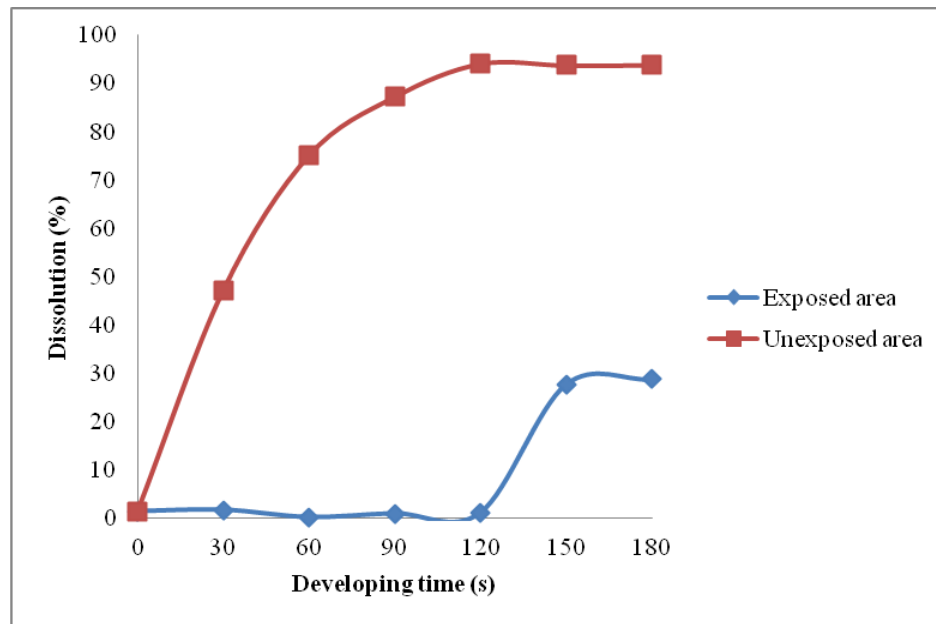


**Figure 5.7** The relation between % dissolution of the exposed and unexposed areas of polyimide films in the developing solvent with each developing time

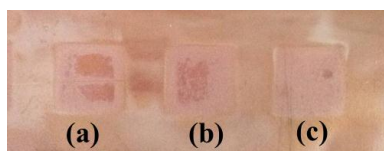
#### 5.4 Determination of the relation between area openings of negative photosensitive polyimide films with photo-mask size

The area openings of negative photosensitive polyimide films were determined by Stylus Profiler then sizes of the photo-mask used in these researches were 5x5, 4x4, 3x3 and 2x2 mm or the areas of the photo-mask are 25, 16, 9 and 4 mm<sup>2</sup>, respectively, which photo-mask was used for unexposed UV area. The total results of the opening ratio of negative photosensitive polyimide films with photo-mask would be investigated are as follows

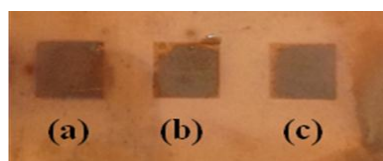
$$\text{Ratio area opening of NPSPI films} = \frac{\text{Area of opening}}{\text{Area of photomask}}$$

**Table 5.5** The ratio area opening of NPSPI films with photo-mask size 5x5 mm

Position	Size of opening (mm)	Area of opening (mm <sup>2</sup> )	Area of photo-mask (mm <sup>2</sup> )	Ratio area of opening
(a)	4.71x4.58	21.57	25.00	0.86
(b)	4.82x4.69	22.61	25.00	0.90
(c)	4.95x4.74	23.46	25.00	0.94
<b>Average</b>		22.55	25.00	0.90
<b>Standard deviation</b>		0.95	0	0.04

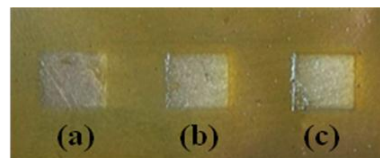
**Figure 5.8** Position of the area opening of NPSPI films with photo-mask size 5x5 mm**Table 5.6** The ratio area opening of NPSPI films with photo-mask size 4x4 mm

Position	Size of opening (mm)	Area of opening (mm <sup>2</sup> )	Area of photo-mask (mm <sup>2</sup> )	Ratio area of opening
(a)	3.98x4.00	15.92	16.00	0.99
(b)	3.89x3.90	15.52	16.00	0.97
(c)	3.99x3.96	15.96	16.00	0.99
<b>Average</b>		15.80	16.00	0.98
<b>Standard deviation</b>		0.24	0	0.01

**Figure 5.9** Position of the area opening of NPSPI films with photo-mask size 4x4 mm

**Table 5.7** The ratio area opening of NPSPI films with photo-mask size 3x3 mm

Position	Size of opening (mm)	Area of opening (mm <sup>2</sup> )	Area of photo-mask (mm <sup>2</sup> )	Ratio area of opening
(a)	2.46x2.74	6.74	9.00	0.75
(b)	2.35x2.79	6.56	9.00	0.73
(c)	2.38x2.79	6.64	9.00	0.74
<b>Average</b>		6.65	9.00	0.74
<b>Standard deviation</b>		0.09	0	0.01

**Figure 5.10** Position of the area opening of NPSPI films with photo-mask size 3x3 mm**Table 5.8** The ratio area opening of NPSPI films with photo-mask size 2x2 mm

Position	Size of opening (mm)	Area of opening (mm <sup>2</sup> )	Area of photo-mask (mm <sup>2</sup> )	Ratio area of opening
(a)	1.95x1.89	3.69	4.00	0.92
(b)	1.94x1.93	3.74	4.00	0.94
(c)	1.94x1.90	3.69	4.00	0.92
(d)	1.97x1.95	3.84	4.00	0.96
<b>Average</b>		3.74	4.00	0.94
<b>Standard deviation</b>		0.07	0	0.02

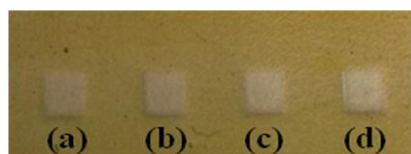


**Figure 5.11** Position of the area opening of NPSPI films with photo-mask size 2x2 mm

**Table 5.9** The ratio area opening of NPSPI/silica hybrid films with photo-mask size 2x2 mm

Position	Size of opening (mm)	Area of opening (mm <sup>2</sup> )	Area of photo-mask (mm <sup>2</sup> )	Ratio area of opening
(a)	1.88x1.89	3.37	4.00	0.84
(b)	1.88x1.83	3.44	4.00	0.86
(c)	1.94x1.87	3.63	4.00	0.91
(d)	1.87x1.82	3.40	4.00	0.85
<b>Average</b>		3.46	4.00	0.87
<b>Standard deviation</b>		0.12	0	0.03

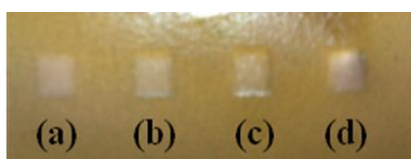


**Figure 5.12** Position of the area opening of NPSPI/silica hybrid films with photo-mask size 2x2 mm

Table 5.5-5.8 shows the opening areas of NPSPI films by Stylus profiler, which showed successful process of developing and position of the area opening of NPSPI films with photo-mask size 5x5, 4x4, 3x3 and 2x2 mm are shown in Figure 5.8-5.11, respectively. The average areas of opening were 22.55, 15.80, 6.65 and 3.74 mm<sup>2</sup> so the average ratio areas of opening were 90, 98, 74 and 94 %, which are

acceptable. The standard deviation of the average areas of opening were 0.95, 0.24, 0.09 and 0.07 then the standard deviation of the average ratio areas of opening were 0.04, 0.01, 0.01 and 0.02, which were narrow enough to have well opened sizes of the desired area. For the ratio area opening of NPSPI/silica hybrid films with photo-mask size 2x2 mm can be shown in Table 5.9 and Figure 5.12. The average area of opening was 3.46 mm<sup>2</sup> or the average ratio area of opening was 87% and the standard deviation of the average area of opening was 0.12 and the standard deviation of the average ratio areas of opening was 0.03, which was acceptable. When compared the ratio area of opening between NPSPI and NPSPI/silica hybrid films with photo-mask size 2x2 mm, the ratio area of opening of NPSPI films was higher than NPSPI/silica hybrid film. However, the degrees of polymerization (DP) of NPSPI/silica hybrid film were higher than NPSPI films (200 Compared to 63, respectively), because NPSPI films could be more easily dissolved in the developing solvents due to lower molecular weight.

### 5.5 Thermal properties

The degradation temperature ( $T_d$ ) estimated from the 5% weight loss of the Thermal Gravimetric Analysis of each system can be showed in Table 5.10 and Figure 5.13

**Table 5.10** The degradation temperature of prepared films after curing at 250 °C

<b>Type of film</b>	<b><math>T_d</math> 5 % (°C)</b>
PI	301.4
NPSPI	269.1
NPSPI/silica hybrid	242.0

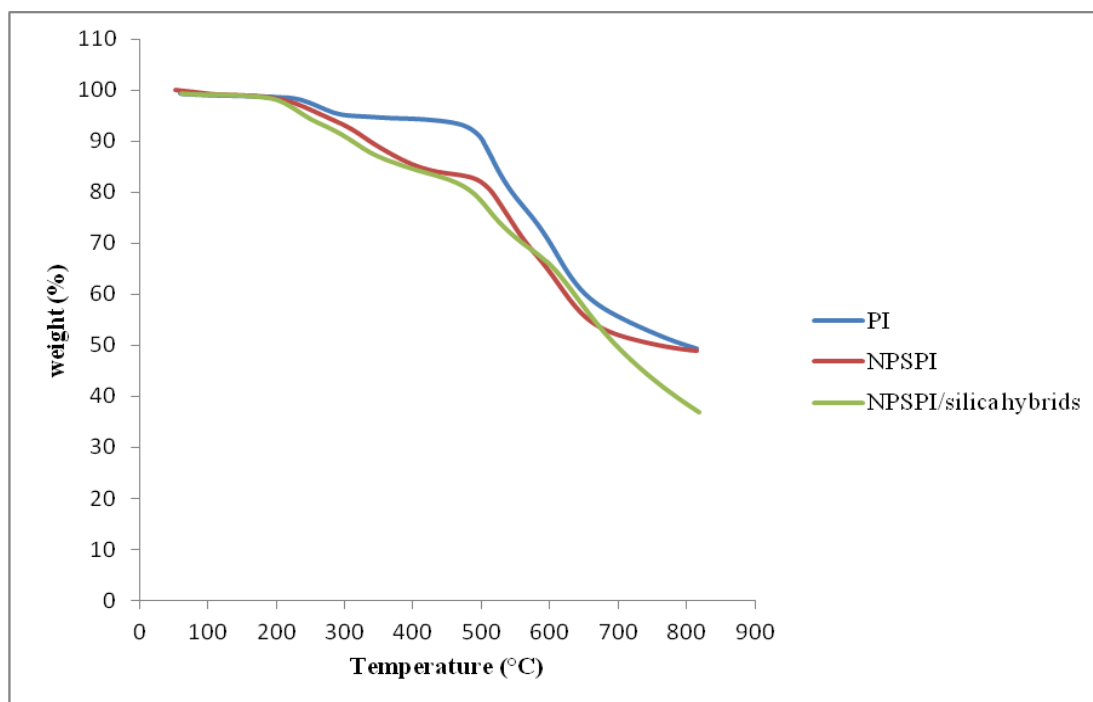


**Figure 5.13** The relation between % weights of polyimide films with temperature

Usually the polyimide can withstand very high temperature by itself and have very high degradation temperature, so polyimide (PI) film had the highest thermal stability. The degradation temperature ( $T_d$ ) 5% weight loss of NPSPI film was lower than PI film because it comprised HEMA as photo precursor which after curing, most of cross-linked polymer would be evaporated away from poly(amic) acid, but some could be remained. For NPSPI/silica hybrid film, it had the lowest thermal stability because vinyl groups in octavinyl POSS molecules, that remained, could be easier decomposition and the higher free volume by the incorporation of POSS in the main chain of NPSPI/silica hybrid film, cause lower resistance to heat. [29-31]

## 5.6 Dielectric properties

The dielectric properties of the polyimide films were investigated by LCR meter. Table 5.11 shows the dielectric constants of the polyimide films, which can be calculated from the following equation;

$$k = \frac{Ct}{\epsilon_0 A}$$

Where  $C$  is the measured capacitance,  $t$  is the thickness of the sample,  $A$  is the area of the hybrid films,  $\epsilon_0$  is the permittivity of the free space (8.854 pF/m).

**Table 5.11** Dielectric constant of polyimide films each system

Type of film	Thickness ( $\mu\text{m}$ )	Area ( $\text{cm}^2$ )	Capacitance (pF)	Dielectric constants (k)
PI	108	1.4x1.8	124.43	6.02
NPSPI	131	2.0x2.0	117.33	4.34
NPSPI/silica hybrid	85	2.1x2.0	94.12	2.16

Table 5.11 shows the reduction of the dielectric constant according to the incorporation of POSS in the main chain of NPSPI/silica hybrid films because the lower dielectric constant of POSS molecules and the higher free volume caused by POSS molecules. The dielectric constant of NPSPI/silica hybrid was remarkable because of it was lower than 2.5, which is the required dielectric constant for high density of circuit films. When compared to the work by S.Srisuwan et.al. [13], this dielectric is lower than what they had done (the lowest dielectric constant of PI/silica hybrid film they obtained was 2.31), which showed the more successful of this project.

## 5.7 Tensile properties

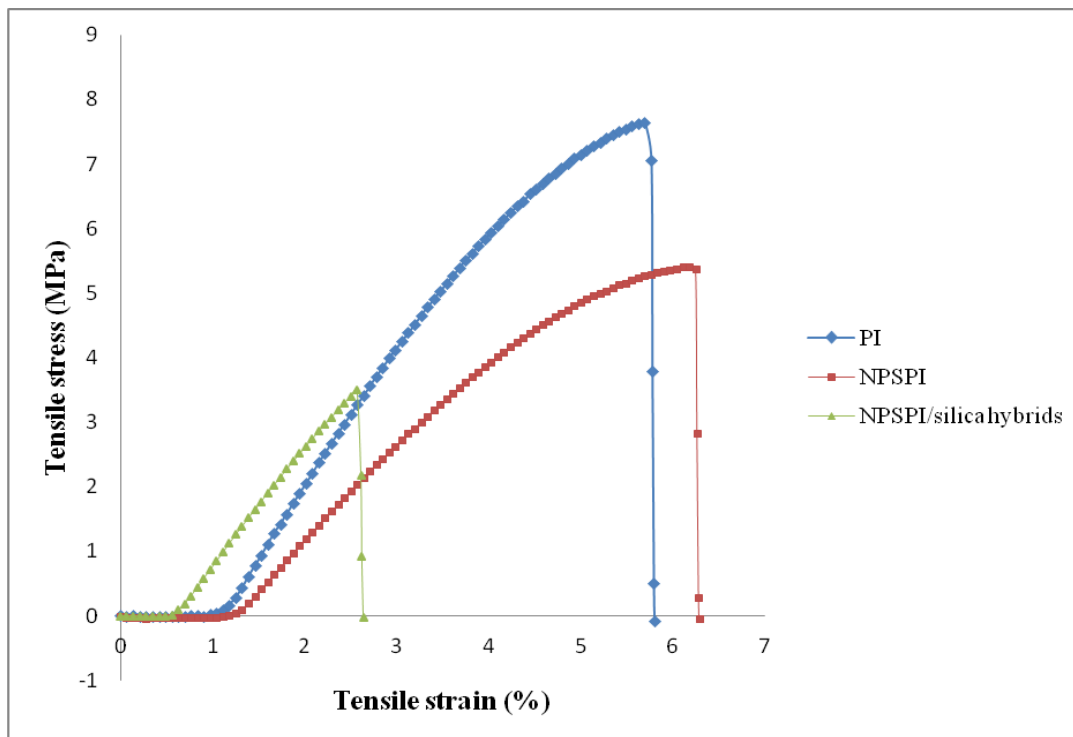


**Figure 5.14** Tensile strengths of PI, NPSPI and NPSPI/silica hybrid films

**Table 5.12** Tensile properties of PI, NPSPI and NPSPI/silica hybrid films

Type of film	Tensile stress at break	Tensile strain at break
	(kPa)	(%)
PI	7,060	5.76
NPSPI	5,380	6.25
NPSPI/silica hybrid	2,180	2.61

The results of tensile stress tests of the films can be shown in Figure 5.14 and Table 5.12. The NPSPI/silica hybrid film had the lowest tensile stress, because of the higher free volume due to the incorporation of POSS in the main chain PI. This was possible reason for the weakness of the NPSPI/silica hybrid film. The normal Kapton will have the tensile strength in the ranges of 200 MPa which are 30, 40 and 90 times larger than the tensile strength of the PI, NPSPI and NPSPI/silica hybrid films,



respectively, because Kapton made from different monomer than these PI in this research. However, this weak point might be less important if the NPSPI/silica hybrid film was laid on higher tensile strength film and the monomer that were comprised in NPSPI was designed for highest adhesion to substrate, not the tensile strength.

### 5.8 Volume shrinkage of films

The film was dried at 55 °C for 2 hours and cured by the multi-step heating process of 100, 150, 200 and 250 °C for 30 min each in the vacuum oven. The thickness of various temperatures and the volume shrinkage of the prepared films after curing at 250 °C of all systems in this research can be shown in Table 5.13. The volume shrinkage of prepared films could be determined from the following equation;

$$\text{Volume shrinkage (\%)} = \frac{\text{Initial Thickness} - \text{Thickness after curing at } 250^{\circ}\text{C}}{\text{Initial thickness}} \times 100$$

**Table 5.13** The volume shrinkage of prepared films after curing at 250 °C

Type of film	Thickness at various temperature (µm)					Volume Shrinkage (%) at 250 °C
	55 °C	100 °C	150 °C	200 °C	250 °C	
PI	33.40	31.33	28.65	26.50	20.43	38.83
NPSPI	28.10	21.50	19.20	17.70	12.60	55.16
NPSPI/silica hybrid	26.00	20.13	18.30	17.50	13.75	47.12

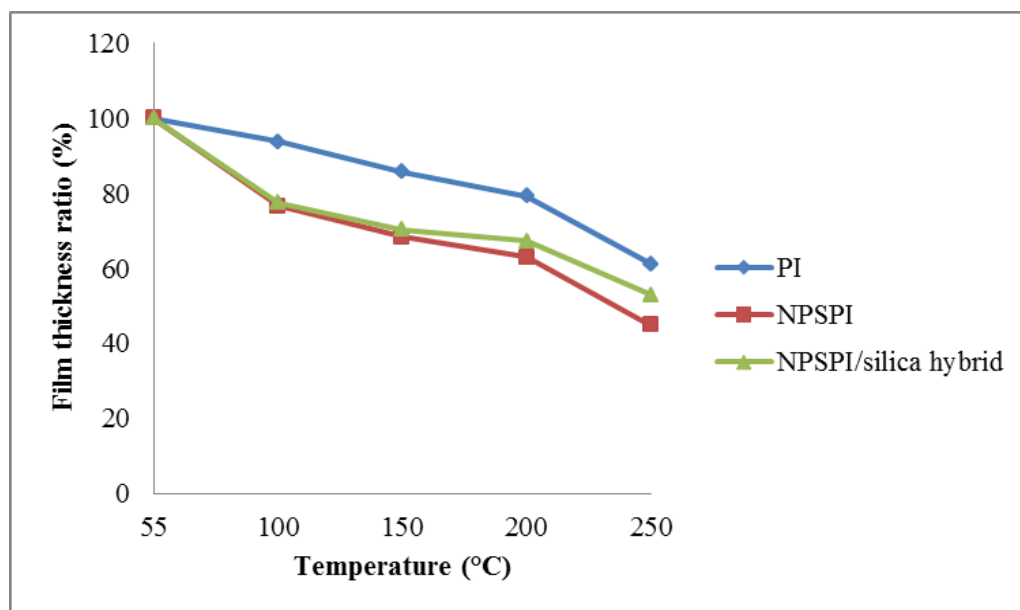


**Figure 5.15** Thickness variations of PI, NPSPI and NPSPI/silica hybrid films in the curing process

Figure 5.15 shows the variation of thickness of the polyimide films at different curing temperatures. The lower thickness results from the loss of small molecules at each temperature. At first, the solvent was lost from the system at lower temperature. The water from poly(amic) acid that changes to be polyimide could be more identified at higher temperature. The ratios of film thickness after curing at 250 °C are 61, 45, 53 % (volume shrinkage are 39, 55 and 47 %) for PI, NPSPI and NPSPI/silica hybrid films, respectively. From these results, the volume shrinkage of the NPSPI/silica hybrid systems were lower than the volume shrinkage of the NPSPI systems but still higher than PI systems. The thickness losses of NPSPI films were higher than PI film (at the same conditions) due to the loss of photo-cross-linking agents, 2-hydroxyethyl methacrylate (HEMA) and Irgacure-819, after cured but the cooperation of octavinyl POSS of NPSPI/silica hybrid film could reduce the shrinkage of negative photosensitive polyimide about 8 percent because the octavinyl POSS was cross-linked with HEMA, thus after cured, the loss of HEMA molecules was less than NPSPI system.

### 5.9 Morphology of negative photosensitive polyimide films



(a)



(b)

**Figure 5.16** Photograph of NPSPI films (a) from Mobile phone (b) from Optical microscope

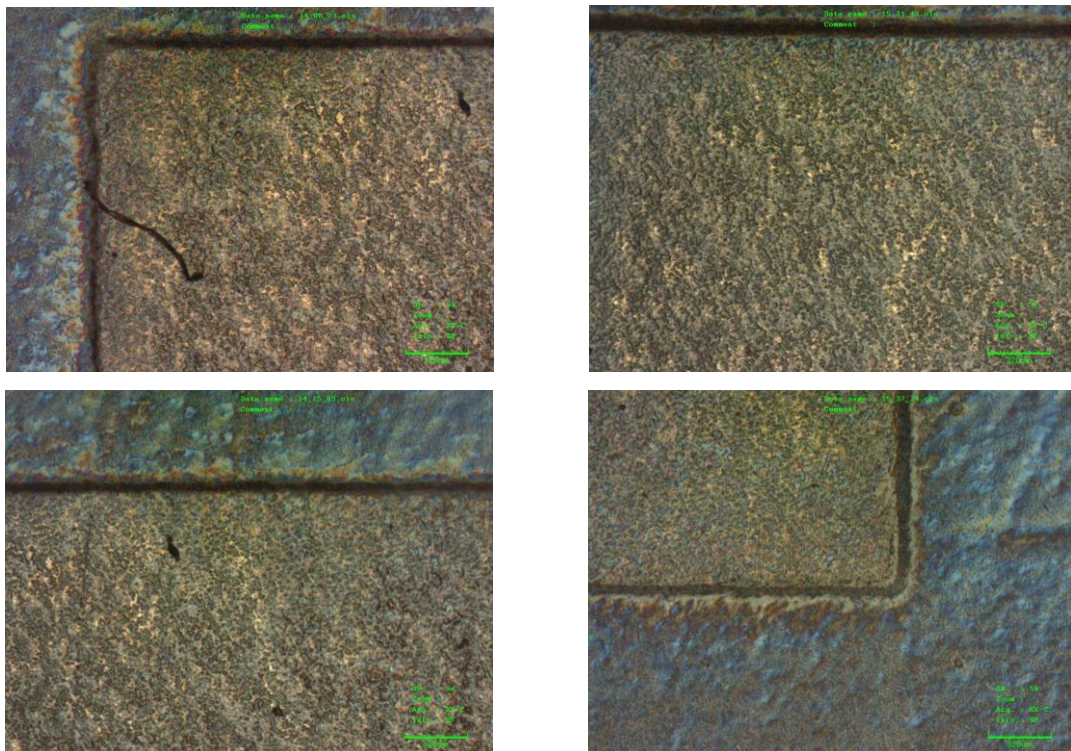


**Figure 5.17** Morphology of NPSPI films on copper foil. [Size of opening of 2x2 mm]

Figure 5.16 shows the photograph of the developed pattern of NPSPI films. The unexposed areas were not exposed to UV light. After developed, the films were dissolved by the solvent that washed away the unexposed part. The areas that exposed to the UV light were not easily dissolved by the solvent when developed, so the films remained thick after cure. To clarify that the unexposed areas were really washed away, so the developed pattern of NPSPI films were characterized by confocal microscope as shown in Figure 5.17. The morphology of the NPSPI films were measured by Confocal Microscope with magnification 5x. The rectangular patterns at 2x2 mm were rather clearly observed, but had a few deformations or incomplete dissolved at the corners (not a sharp corner). The reasons for the incomplete dissolved of the unexposed areas might due to the too short developed time or the too long exposed time and might be due to diffusion of Irgacure radicals from the exposed area, which hardly be controlled.

## **CHAPTER VI**

### **CONCLUSIONS & RECOMMENDATIONS**

#### **6.1 Conclusions**

In this research, the synthesis of negative photosensitive polyimides, negative photosensitive polyimide/silica (POSS) hybrid materials, the controlled thickness (about 12.5 micron) and the relation between area opening of negative photosensitive polyimide films with photo-mask size and the properties of negative photosensitive polyimide films were investigated.

##### **6.1.1 Synthesis of the negative photosensitive polyimide and negative photosensitive polyimide/silica (POSS) hybrid materials**

The negative photosensitive polyimide and negative photosensitive polyimide/silica (POSS) hybrid materials were synthesized using the two-step method polymerization and by incorporating click chemistry based on 4-Aminobenzenethiol and Octavinyl POSS at end molecule of polyimide were studied. A number of conclusions may be summarized as follows:

1. From FTIR spectrum, it indicated the structure of polyimide, photosensitive polyimide and incorporation of octavinyl POSS in photosensitive polyimide structure.
2. From <sup>1</sup>H-NMR, it indicated the 4-aminobenzenethiol was incorporated with Octavinyl POSS.
3. From thickness measurements, the negative photosensitive polyimide films with the thickness approximately controlled at 12.5 micron were successfully prepared.
4. From effect of developing time on the dissolution in the developer of the negative photosensitive polyimide films, at developing time of 120 second was the best condition because the unexposed areas were completely washed away with the developing solvent more than other conditions so % dissolution of polyimide films in the developing solvent was the highest. (94.12 %)

5. From the area opening of negative photosensitive polyimide films with photo-mask size, the area opening of NPSPI films of 2x2 mm were successfully prepared and the ratio area of opening was 94 % which is acceptable.

6. From dielectric constant, by incorporation octavinyl POSS can decrease dielectric constant of negative photosensitive polyimide ( $k = 2.16$ ).

7. From volume shrinkage of films measurements, the shrinkage of the final negative photosensitive polyimide can be reduced about 8 percent by the addition of octavinyl POSS in the end-chains.

8. From Tensile measurements, the highest possible tensile strength of NPSPI/silica hybrid film was 2.18 MPa, which was too low. However, the formula of NPSPI was designed for the highest adhesion to surface of copper, not the tensile strength and if the NPSPI/silica hybrid is adhered to high tensile strength substrate (LPI4), this problem of lower tensile strength will be diminished.

## **6.2 Recommendations**

6.2.1 There should be more investigation in the properties of the 2-hydroxyethyl methacrylate (HEMA) photosensitive precursor and Bis(2,4,6-trimethylbenzoyl)phenyl phosphine oxide (Irgacure-819) photosensitive initiator in order to check that HEMA and Irgacure-819 can really absorb in the wavelength of U.V. radiation.

6.2.2 The more improvement of thermal and tensile properties of negative photosensitive polyimide should be investigation in the future. However, the high adhesion properties should maintained.

## REFERENCES

- [1] Hong Zhuang. Synthesis and Characterization of Aryl Phosphine Oxide Containing Thermoplastic Polyimides and Thermosetting Polyimides with controlled Reactivity. Blacksburg, Virginia. (1998):15.
- [2] Seunghyuk Choi, Seokkyu Lee, Jihee Jeon, Jaein An, Sher Bahadar Khan, Sangyup Lee, Jongchul Seo and Haksoo Han. A Photoinitiator-Free Photosensitive Polyimide with Low Dielectric Constant. **InterScience** (2010):2937–2945.
- [3] Jay Madigan. **Education Resources from the Science Directorate at NASA Langley Research Center** [Online]. Available from: [http://science-edu.larc.nasa.gov/EDDOCS/Wavelengths\\_for\\_Colors.html](http://science-edu.larc.nasa.gov/EDDOCS/Wavelengths_for_Colors.html). [2012, March 31]
- [4] Peter Cheang, Lorna Christensen and Corinne Reynaga. Optimization of Photosensitive Polyimide Process for Cost Effective Packaging. **Surface Mount Technology Seminar** (1996):1-18.
- [5] Perfecto, Eric D. et al., “Factors That Influence Photosensitive Polyimide Lithography Performance.” ICEMM Proceedings. (1993):40-45.
- [6] Kataoka F, Suzuki H. In: Horie K, Yamashita T, editors. Photosensitive Polyimide. **Lancaster Technomic** (1996).
- [7] Tessler N, Medveder V, Kazes M, Kan S, Banin U. Synthesis and properties of new polyimide–silica hybrid films through both intrachain and interchain bonding. **Science** 295(2002):1506.
- [8] Sysel P, Pulec R, Maryska M. Preparation and properties of poly (imide siloxane) segmented copolymer/silica hybrid nanocomposites. **Polym J** 29(1997):607.
- [9] Chen Y, Iroh JO. Synthesis and Characterization of Polyimide/Silica Hybrid Composites. **Chem Mater** 11(1999):1218.
- [10] Ahmad Z, Mark JE. Preparation and characterization of polyimide/silica nanocomposite spheres. **Chem Mater** 13(2001):3320.

- [11] Ken-ichi FUKUKAWA, Mitsuru UEDA. Recent Progress of Photosensitive Polyimides. **Polymer Journal** 40(2008):281-296.
- [12] Chang CC, Wei KH, Chen WC. Spin-Coating of Polyimide-Silica Hybrid Optical Thin Films. **J Electrochem Soc** 150(2003):147.
- [13] Suttisak Srisuwan, Supakanok Thongyai, Piyasan Praserttham. Synthesis and Characterization of Low-Dielectric Photosensitive Polyimide/Silica Hybrid Materials. **InterScience** 117(2010):2422–2427.
- [14] Sroog C. E., Endrey A. L., Abroma S. V., Berr C. E., Edward W. M., and Oliver K. L. Aromatic polypyromellitimides from aromatic polyamic acids. **J Polym Sci** 3(1965): 1373.
- [15] Vinogradova, S.V., Vygodskii, Y.S. and Korshak, V.V. **Polym Sci USSR** 12(9)(1970): 2254.
- [16] Takekoshi T., Ghosh M.K. and Mittal K.L. Polyimides-Fundamentals and Applications. New York: **Marcel-Dekke** (1996).
- [17] Ghosh MK and Mittal KL. Polyimides-Fundamentals and Applications. New York: **Merced-Dekker** (1996).
- [18] Harris F.W., Wilson D., Stenzenberger H.D, Hergenrother P.M., Chapman and Hall. Polyimides. New York: (1990).
- [19] Pravednikov A.N., Kardash I.Y., Glukhoyedov N.P. and Ardashnikov A.Y. **Polym Sci USSR** 15(2)(1973): 399.
- [20] Data from Materials for Polyimide Synthesis, TCl.
- [21] C. E. Sroog. **Progress of polymer science polyimides** 16(1991):625-665.
- [22] CIBA. **Education photoinitiator** [Online]. Available from: <http://www.ciba.com/photoinitiator.htm>. [2012, March 31]
- [23] C. Franklin et. al., “Polyimide Evaluations for Controlled Collapse Chip Connection and Passivation Stress Buffer Technologies”. OCG Microlithography Seminar. **Interface’93 Proceedings** (1993):91-104.
- [24] Le Thu T. Nguyen, et al. Synthesis and characterization of a photosensitive polyimide precursor and its photocuring behavior for lithography applications. **Optical Materials** 29(2007):610-618.
- [25] Jung M.-S, Joo W.-J, Choi B.-K, Jung H.-T. **Polymer** 47(2006):6652.



- [26] Warren W. Flack, Gary E. Flores, Lorna Christensen and Gary Newman. An Investigation of the Properties of Photosensitive Polyimide Films. **SPIE** 27(1996):26-75.
- [27] Steve Lien-Chung Hsu and Ming Hsin Fan. Synthesis and Characterization of Novel Negative-Working Aqueous Base Developable Photosensitive Polyimide Precursors. **Polymer** 45(2004):1101-1109.
- [28] Seunghyuk Choi, Seokkyu Lee, Jihee Jeon, Jaein An, Sher Bahadar Khan, Sangyup Lee, Jongchul Seo and Haksoo Han. A Photoinitiator-Free Photosensitive Polyimide with Low Dielectric Constant. **Inc J Appl Polym Sci** 117(2010):2937-2945.
- [29] Yu-Wen Wang, Cheng-Tyng Yen, Wen-Chang Chen. Photosensitive Polyimide/Silica Hybrid Optical Material: Synthesis, Properties and Patterning. 46(2005):6959-6967.
- [30] Yang-Yen Yu. Synthesis and Optical Properties of Photosensitive Polyimide/Silica Hybrid Thin Films. **Materials Chemistry and Physics** 113(2009):567-573.
- [31] Yu-Wen Wang and Wen-Chang Chen. New photosensitive colorless polyimide-silica hybrid optical materials: Synthesis, properties and patterning. **Materials Chemistry and Physics** 126(2011):24-30.
- [32] Chao Zhang, Hong Yao Xu and Xian Zhao. Structure and properties of low-dielectric-constant poly(acetoxystyrene-co-octavinyl polyhedraloligomeric silsesquioxane) hybrid nanocomposite. **Chinese Chemical Letters** 21(2010):488–491.
- [33] SDBS. **Spectral Database for Organic Compounds SDBS** [Online]. Available from: <http://sdb.sriodb.aist.go.jp>. [2013, April 16]
- [34] D Gnanasekaran, K Madhavan and B S R Reddy. Developments of polyhedral oligomeric silsesquioxanes (POSS), POSS nanocomposites and their applications: A review. **Journal of Scientific & Industrial Research** 68(2009):437–464.

- [35] Benhong Yang, Jirong Li, Jiafeng Wang, Hongyao Xu, Shangyi Guang and Cun Li. Poly(vinyl pyrrolidone-co-octavinyl polyhedral oligomeric silsesquioxane) Hybrid Nanocomposites: Preparation, Thermal Properties, and Tg Improvement Mechanism. **InterScience** (2008):2963–2969.
- [36] Benhong Yang, Jirong Li, Jiafeng Wang, Hongyao Xu, Shangyi Guang and Cun Li. Preparation and Thermal Property of Hybrid Nanocomposites by Free Radical Copolymerization of Styrene with Octavinyl Polyhedral Oligomeric Silsesquioxane. **InterScience** (2007):320-326.
- [37] Yu Gao, Chuanglong He, Yangen Huang and Feng-Ling Qing. Novel water and oil repellent POSS-based organic/inorganic nanomaterial: Preparation, characterization and application to cotton fabrics. **Polymer** 51(2010):5997-6004.
- [38] Anja S. Goldmann, Andreas Walther, Leena Nebhani, Raymond Joso, Dominique Ernst, Katja Loos, Christopher Barner-Kowollik, Leonie Barner and Axel H. E. Muller. Surface Modification of Poly(divinylbenzene) Microspheres via Thiol-Ene Chemistry and Alkyne-Azide Click Reactions. **Macromolecules** (2009).

## APPENDICES

## APPENDIX A

### STYLUS PROFILER MEASUREMENT

Stylus profiler diagrams of negative photosensitive polyimide (NPSPI) films with photo-mask size 2x2 mm

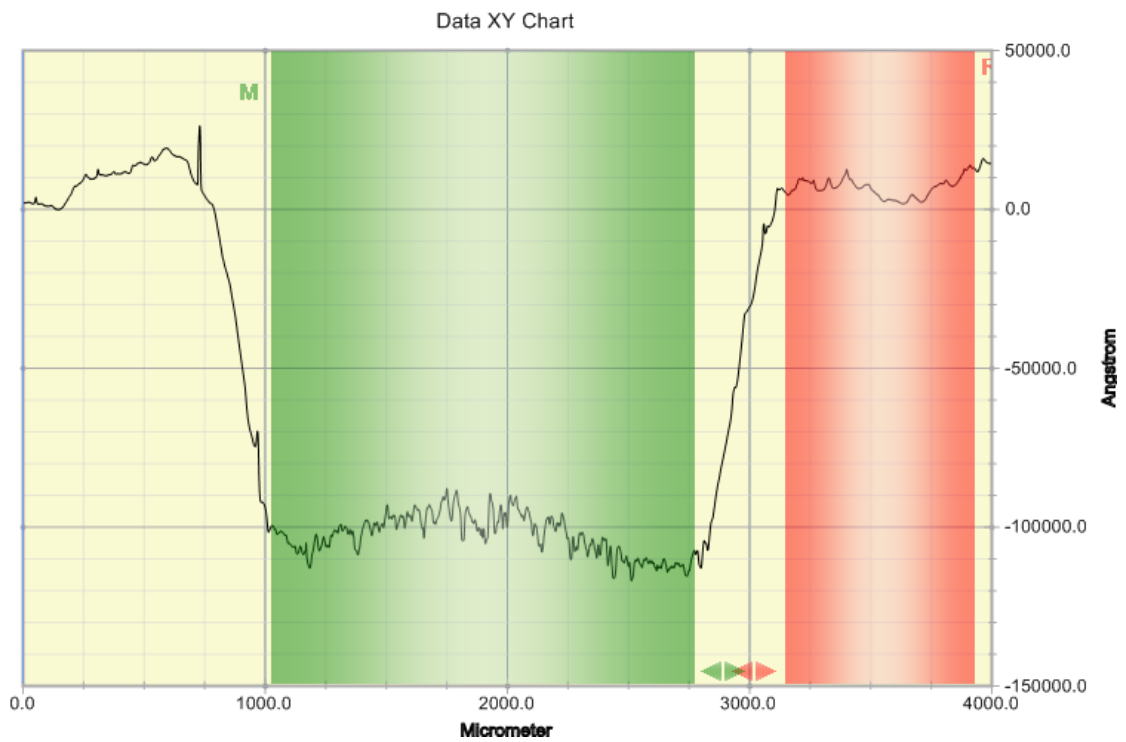
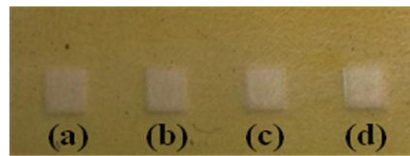


**Figure A-1** Stylus profiler diagrams of NPSPI films with photo-mask size 2x2 mm at position (a)

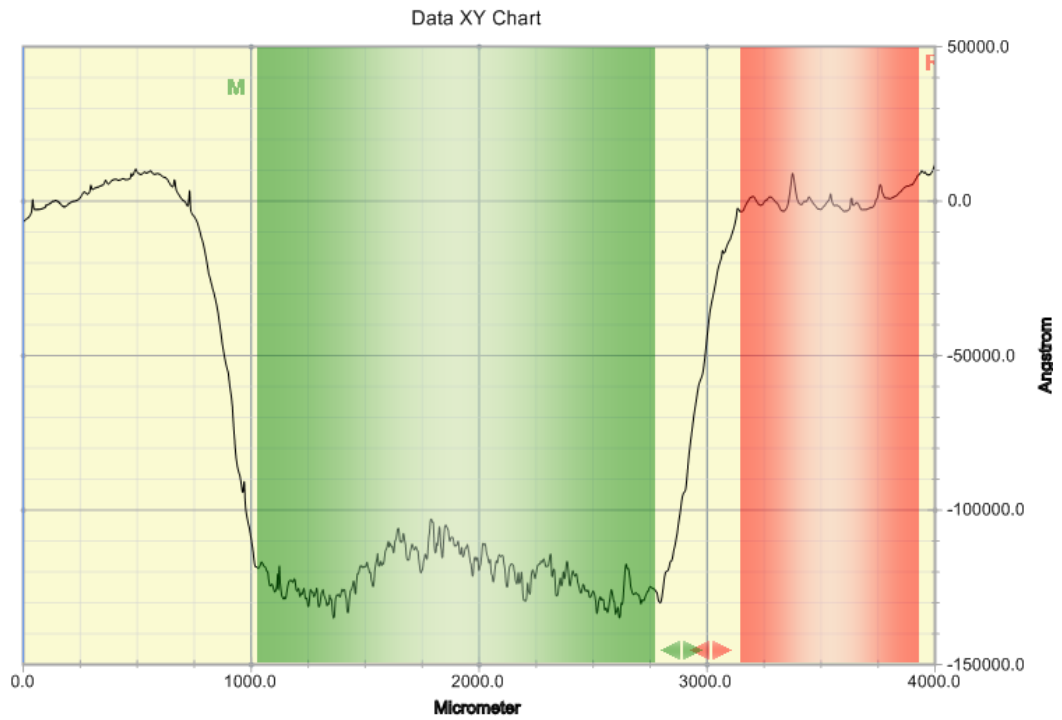


**Figure A-2** Stylus profiler diagrams of NPSPI films with photo-mask size 2x2 mm at position (b)

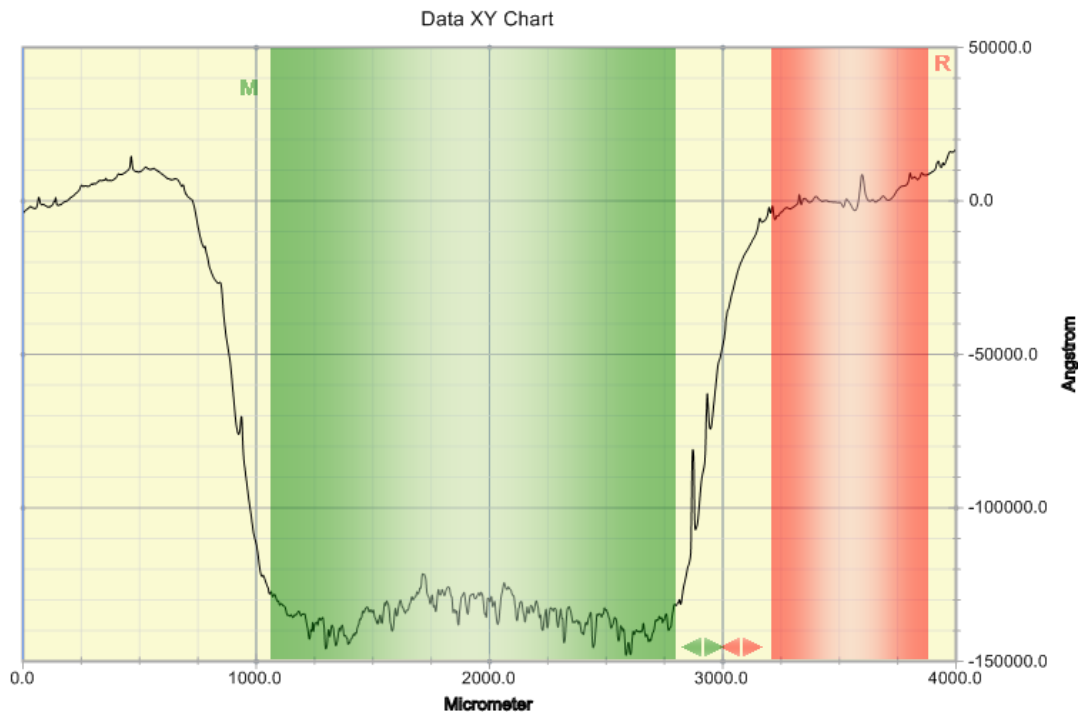


**Figure A-3** Stylus profiler diagrams of NPSPI films with photo-mask size 2x2 mm at position (c)

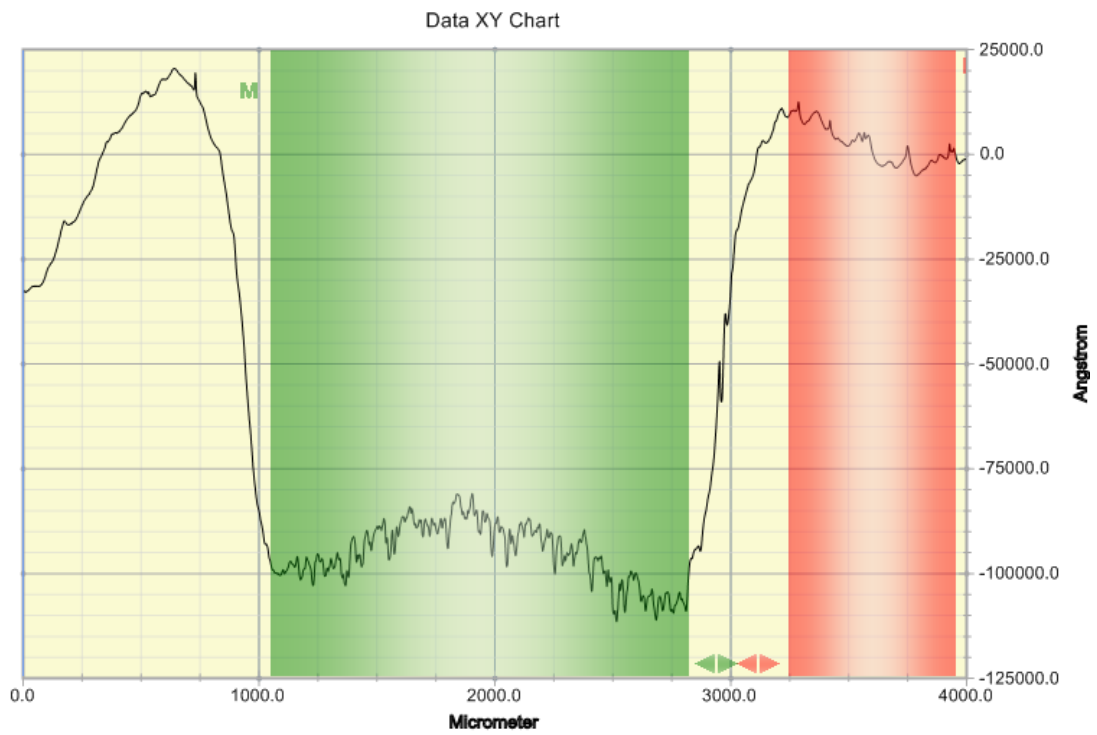


**Figure A-4** Stylus profiler diagrams of NPSPI films with photo-mask size 2x2 mm at position (d)

**APPENDIX B**  
**THERMOGRAVIMETRIC ANALYSIS (TGA)**  
**CHARACTERIZATION**

TGA diagrams of polyimide (PI), negative photosensitive polyimide (NPSPI) and negative photosensitive polyimide/silica hybrids (NPSPI/silica hybrids) films.

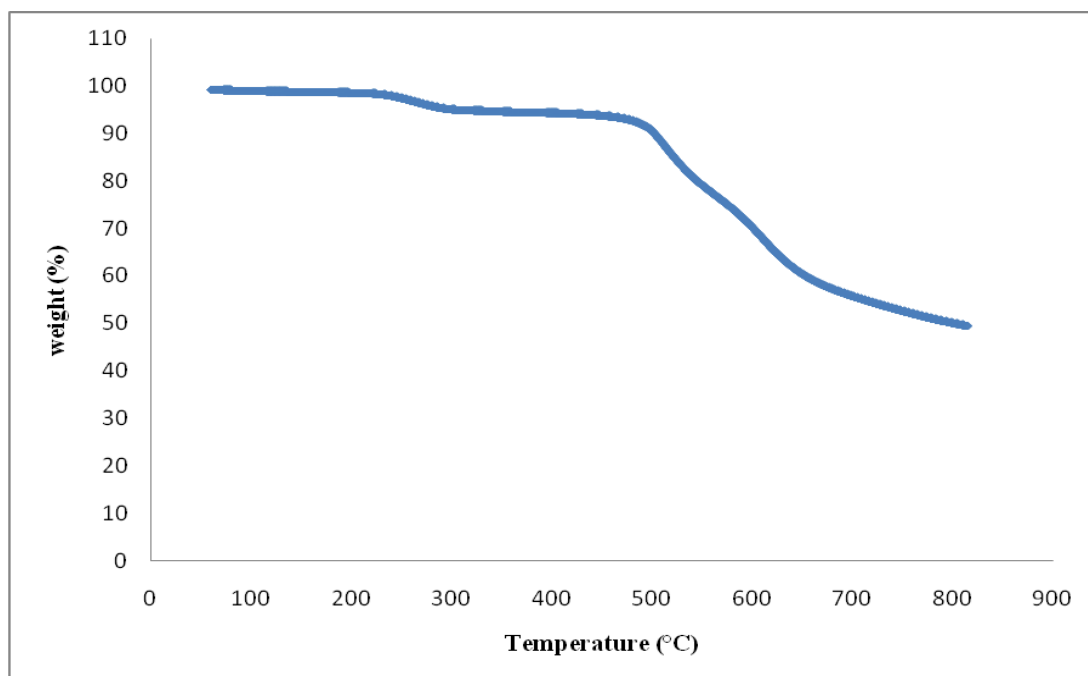


**Figure B-1** Thermogravimetric analysis of PI films at rate 10 °C/min, in N<sub>2</sub>

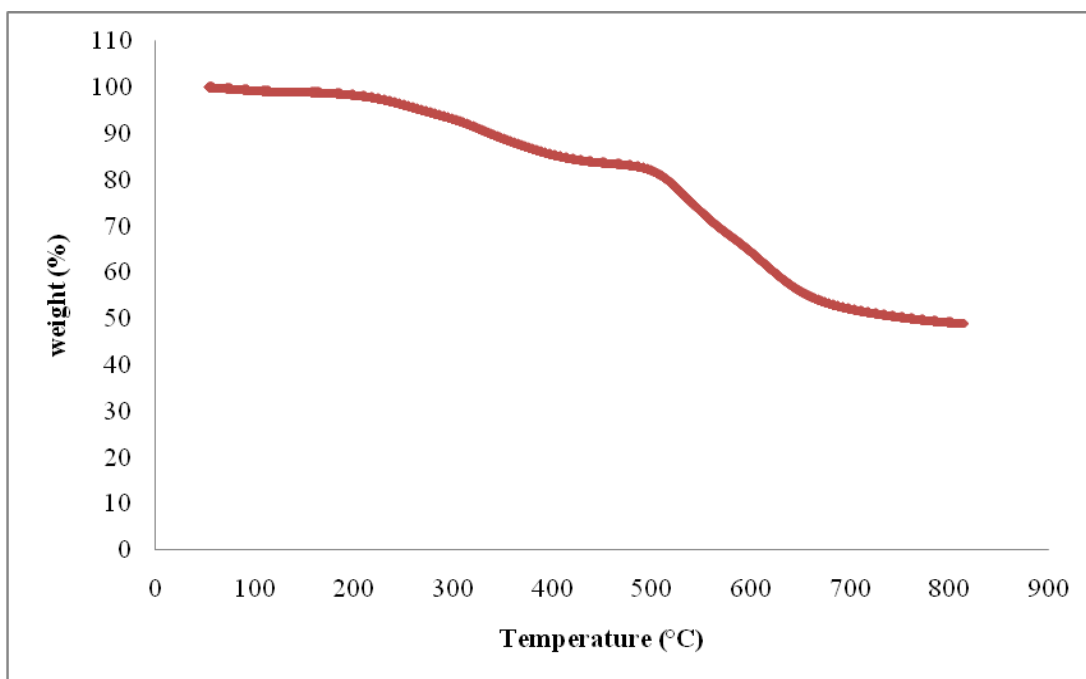


**Figure B-2** Thermogravimetric analysis of NPSPI films at rate 10 °C/min, in N<sub>2</sub>

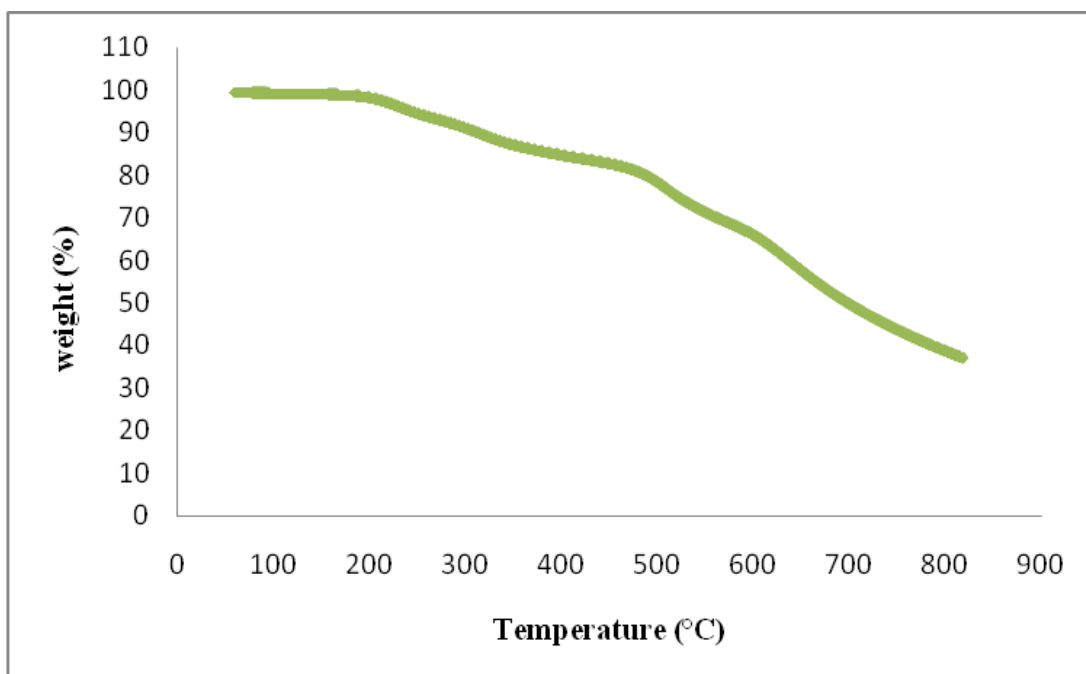


**Figure B-3** Thermogravimetric analysis of NPSPI/silica hybrids films at rate 10 °C/min, in N<sub>2</sub>



## APPENDIX C

### TENSILE PROPERTIES CHARACTERIZATION

Tensile diagrams of polyimide (PI), negative photosensitive polyimide (NPSPI) and negative photosensitive polyimide/silica hybrids (NPSPI/silica hybrids) films.

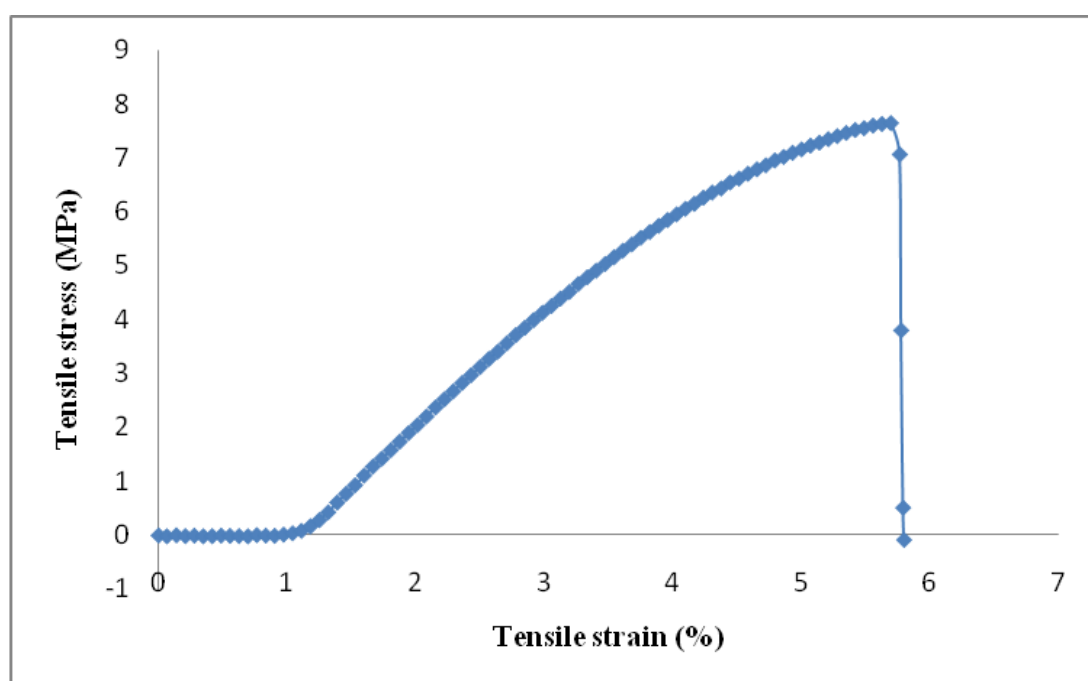


**Figure C-1** Tensile strengths of PI films at 5.76% of tensile strain at break

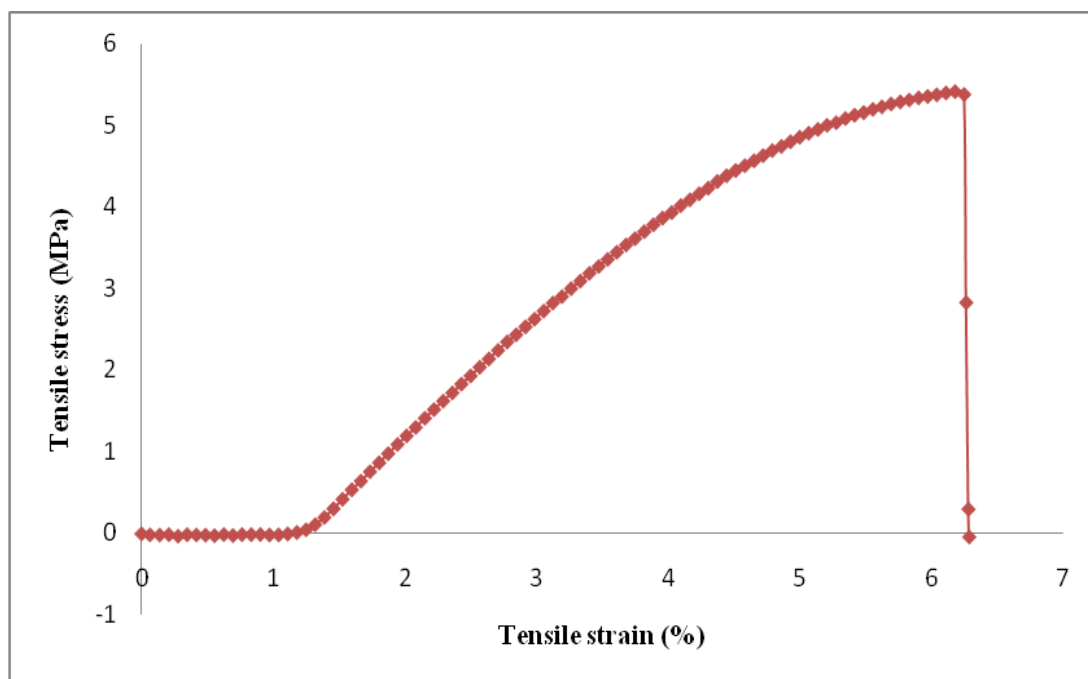


**Figure C-2** Tensile strengths of NPSPI films at 6.25% of tensile strain at break

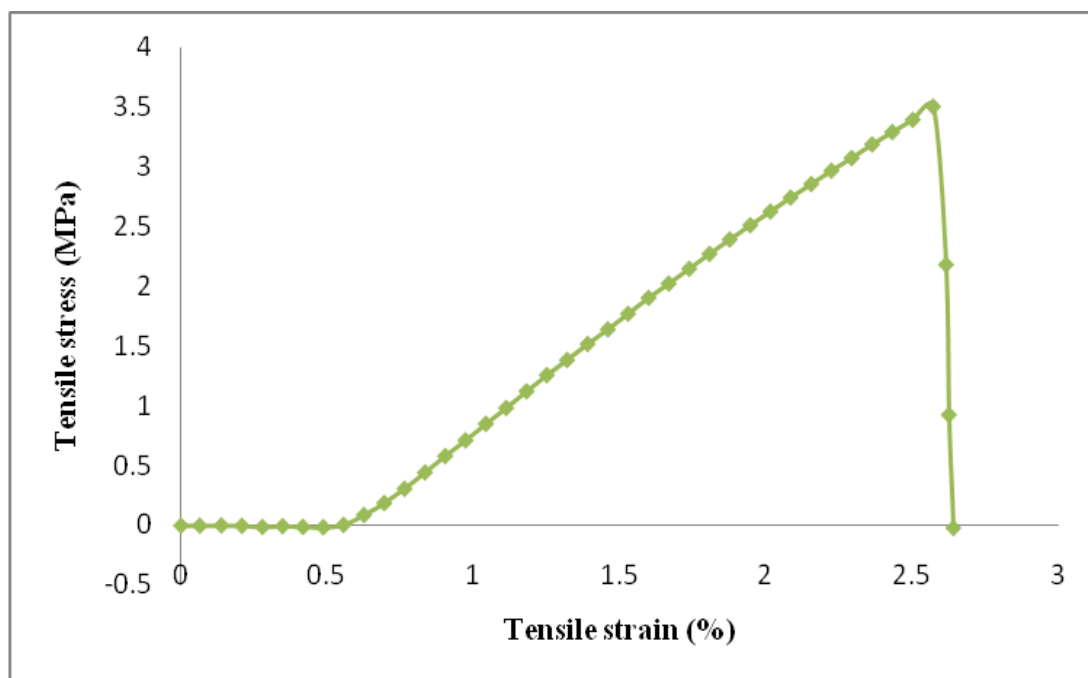


**Figure C-3** Tensile strengths of NPSPI/silica hybrids films at 2.61% of tensile strain at break

## VITA

Miss Noppamas Wutikunprapan was born on November 15, 1988 in Pichit, Thailand. She graduated the bachelor's degree in Chemical Engineering from Department of Chemical Engineering, Faculty of Engineering, King Mongkut's Institute of Technology Ladkrabang on May 2011 with GPA of 3.14. She entered the Master of Engineering in Chemical Engineering at Chulalongkorn University on June, 2011. She has been accepted for publication in the book of proceeding of Pure and Applied Chemistry International Conference 2013 in the topic of "Synthesis and Characterization of ultra-thick negative photosensitive polyimide" which was held in January 23-25, 2013 at The Tide Resort, Chonburi, Thailand. She graduated the master's degree on May 2013 with GPA of 3.65.